Phytomedicine 131 (2024) 155786

Contents lists available at ScienceDirect

Phytomedicine

journal homepage: www.elsevier.com/locate/phymed

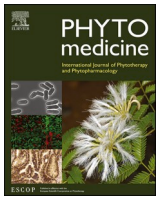

Original Article

The role of the natural compound naringenin in AMPK-mitochondria modulation and colorectal cancer inhibition

Dan Wang [a,1], Yue Zhou [a,1], Li Hua [a], Meichun Hu [a], Ni Zhu [a], Yifei Liu [b,*], Yanhong Zhou [a,*]

[a] School of Basic Medical Sciences, Xianning Medical College, Hubei University of Science and Technology, Xianning, Hubei 437100, China
[b] School of Biomedical Engineering and Imaging, Xianning Medical College, Hubei University of Science and Technology, Xianning, Hubei 437100, China

ARTICLE INFO

Keywords:
Colorectal cancer
Naringenin
Mitochondria
AMPK
Mouse model
Apoptosis

ABSTRACT

Background: Although AMP-activated protein kinase (AMPK) has been extensively studied in cellular processes, the understanding of its substrates, downstream functions, contributions to cell fate and colorectal cancer (CRC) progression remains incomplete.
Purpose: The aim of this study was to investigate the effects and mechanisms of naringenin on CRC.
Methods: The biological and cellular properties of naringenin and its anticancer activity were evaluated in CRC. In addition, the effect of combined treatment with naringenin and 5-fluorouracil on tumor growth in vitro and in vivo was evaluated.
Results: The present study found that naringenin inhibits the proliferation of CRC and promote its apoptosis. Compared with the naringenin group, naringenin combined with 5-fluorouracil had significant effect on inhibiting cell proliferation and promoting its apoptosis. It is showed that naringenin activates AMPK phosphorylation and mitochondrial fusion in CRC. Naringenin combined with 5-fluorouracil significantly reduces cardiotoxicity and liver damage induced by 5-fluorouracil in nude mice bearing subcutaneous CRC tumors, and attenuates colorectal injuries in azoxymethane/DSS dextran sulfate (AOM/DSS)-induced CRC. The combination of these two drugs alters mitochondrial function by increasing reactive oxygen species (ROS) levels and decreasing the mitochondrial membrane potential (MMP), thereby stimulating AMPK/mTOR signaling. Mitochondrial dynamics are thereby regulated by activating the AMPK/p-AMPK pathway, and mitochondrial homeostasis is coordinated through increased mitochondrial fusion and reduced fission to activate apoptosis in cancer cells.
Conclusions: Our data suggest that naringenin is important for inhibiting CRC proliferation, possibly through the AMPK pathway, to regulate mitochondrial function and induce apoptosis in CRC.

Introduction

Colorectal cancer (CRC) is a malignant tumor that occurs in the colon or rectum (Siegel et al., 2023a). At present, surgery can no longer achieve a cure for CRC patients who have experienced recurrence or metastasis after clinical radical resection of CRC tumors (Hsu et al., 2023). In clinical practice, a new adjuvant treatment based on 5-fluorouracil is recommended for CRC patients with high-risk factors (Huang et al., 2022). The medicine 5-fluorouracil is very important for treating different kinds of cancer. 5-Fluorouracil has serious cardiotoxic side effects during application, which are usually characterized by myocardial ischemia but also often present with clinical symptoms such as arrhythmia, pericarditis, and heart failure, which can lead to death in severe cases (Hu et al., 2020). Natural compound drugs have shown potent anticancer effects on both experimental and clinical models and may serve as alternative chemotherapeutic agents for CRC treatment (Chen et al., 2023). However, our understanding of the precise mechanism by which natural drugs promote cancer cell apoptosis and dysfunction is still in its infancy.

Over time, eating mostly plants has been shown to help stop cancer

Abbreviations: CRC, colorectal cancer; AMPK, AMP-activated protein kinase; CIM, chemotherapeutic intestinal mucosal; ROS, reactive oxygen species; DRP1, dynamin-related protein 1; STR, short tandem repeat; IR, inhibitory rate; CI, combination index; SHAPS, shapley additive explanations; SPF, specific pathogen-free; AOM, azoxymethane; DSS, dextran sulfate; IBD, inflammatory bowel disease; HBCDC, Hubei Centers for Disease Control and Prevention; MRI, magnetic resonance imaging; mTOR, mammalian target of rapamycin protein; OMM, outer mitochondrial membrane.

* Corresponding authors.
E-mail addresses: liuyifei@hbust.edu.cn (Y. Liu), zyh@hbust.edu.cn (Y. Zhou).
[1] These authors contributed equally to this work.

https://doi.org/10.1016/j.phymed.2024.155786
Received 11 December 2023; Received in revised form 18 May 2024; Accepted 27 May 2024
Available online 28 May 2024

from forming. Naringenin has been identified as a compound that can hinder the growth and movement of cancer cells, thus impeding the progression of cancer (Wittwer et al., 2023). Research has shown that the use of naringenin alone can mitigate various adverse effects on kidney and heart function, as well as histological structure, in Wistar rats treated with paclitaxel (Khaled et al., 2022). When combined with p-coumaric acid (p-CA), naringenin can help boost antioxidant enzymes in the heart, which protects the heart from damage caused by a drug called DOX (Liu et al., 2022). AMP-activated protein kinase (AMPK) is a crucial regulator of energy metabolism and plays a key role in controlling cell growth and programmed cell death (apoptosis) (Wang et al., 2024). Comprising α, β, and γ subunits, AMPK is a trimeric complex with α subunits existing in two isoforms - α1 and α2. Various studies have highlighted the ability of active components or compounds derived from traditional Chinese medicine to modulate AMPK signaling, thereby influencing the prevention and management of CRC. For instance, flavonoids extracted from Chinese herbs like wogonin (Cheng et al., 2024), tanshinone IIA (Zhu et al., 2022), quercetin (Lu et al., 2023), and cryptotanshinone (Chen et al., 2024) trigger AMPK activation, curb proliferation, and trigger apoptosis in CRC cells.

Furthermore, naringenin exhibits outstanding curative antibacterial, hepatoprotective, cell damage prevention and antioxidant effects on malignant tumors and chronic and metabolic diseases by regulating the levels of ROS (Slika et al., 2022; Xu et al., 2022). The combination of naringenin with chemotherapeutic drugs can increase the cancer cells sensitivity to these chemical, potentially becoming a new cancer therapy (Memariani et al., 2021). Naringenin has antitumor effects on cervical cancer, and the combination of low concentrations of cisplatin and naringenin can improve its effect and make flavonoids potential adjuvants for the treatment of cervical cancer (Martínez-Rodríguez et al., 2020). In addition, the combination of apigenin and naringenin (CoAN) significantly enhances mitochondrial dysfunction, increases oxidative stress, and activates apoptotic pathways compared with apigenin or naringenin alone (Liu et al., 2023). However, studies on the role of naringenin combined with 5-fluorouracil in CRC have not been reported.

Mitochondria play a pivotal role in energy generation, redox balance, metabolic regulation, signaling modulation, cell survival, and proliferation (Hsu et al., 2021). The functionality of mitochondria is under tight control through the processes of fusion and fission, which manage the overall size and connectivity of these organelles (Wai and Langer, 2016). Fusion aids in reducing stress by binding to partially impaired mitochondria to restore their function. Fission is essential for producing new mitochondria and ensuring quality control by eliminating damaged ones. Typically, the absence or reduction of dynamin-related protein 1 (DRP1) leads to a highly interconnected mitochondrial network, whereas the lack of the fusion regulator (i.e., mitochondrial fusion protein 2, MFN2) results in fragmented or aggregated mitochondria (Fenton et al., 2021). Enhanced mitochondrial fission, governed by elevated mitochondrial DRP1 levels and reduced MFN2 expression, promotes cancer growth and spread (Zhang et al., 2023). Thus, mitochondrial fusion and fission counteract each other to regulate the structure and function of mitochondria. Nevertheless, how these processes impact mitochondrial function and cell growth, especially in CRC, necessitates further exploration.

In this work, we reported a previously unrecognized function of naringenin: to activate AMPK signaling and promote mitochondrial fusion to inhibit CRC. In addition, we observed that naringenin combined with 5-fluorouracil interfered more significantly with CRC cells and the AOM/DSS-induced CRC animal model than naringenin or 5-fluorouracil alone. The role of naringenin combined with 5-fluorouracil in activating AMPK-related targets to inhibit CRC was revealed. Finally, we analyzed the regulation of mitochondrial function, and naringenin alone and combined with 5-fluorouracil induced mitochondrial damage in cancer cells by increasing mitochondrial fusion and decreasing mitochondrial fission, ultimately leading to the apoptosis of CRC cells. This study elucidated the effectiveness of naringenin and naringenin combined with 5-fluorouracil in the treatment of CRC.

Materials and methods

Cell culture

The human CRC cell line LoVo was acquired from and characterized by Procell Life Sciences Co., Ltd. (Wuhan, Hubei, China). LoVo cell cultures were sustained in Ham's F-12K media supplemented with 10 % FBS (PM150910B, Wuhan, Hubei, China). LoVo cell were kept warm at 37°Cin a humid environment with a mix of 95 % air and 5 % CO_2. (Thermo Fisher Scientific, USA). None of the cell lines utilized in this study are included in the database of frequently misidentified cell lines maintained by ICLAC. All cell populations were confirmed to be devoid of mycoplasma contamination.

Animal model establishment and treatments

All mice were kept in a dedicated specific pathogen-free (SPF) facility, and all appropriate procedures were carried out in compliance with the Guide for Laboratory Animal Care and Use and authorized by the Ethics Committee of Hubei University of Science and Technology (approval number: 202101011).

In the study involving CRC subcutaneous tumor-bearing animals, 4-week-old male BALB/c-nu mice weighing 16-18 g were sourced from Hunan SJA Laboratory Animal Co., Ltd. For the AOM/DSS orthotopic CRC model, 6-week-old and male BALB/c mice, weighing 18–22 g, were obtained from the Hubei Centers for Disease Control and Prevention (HBCDC). The animal housing facility had adequate ventilation, and the temperature of the mouse housing room is maintained between 18–23 °C and humidity between 40-60 %.

LoVo cells in the logarithmic growth phase were collected, resuspended in PBS to 3×10^7 cells/mL, and 0.2 mL (6×10^6 cells) were injected subcutaneously to the right side of BALB/c-nu mice. Tumor growth was observed every two days after inoculation. Drug intervention was started when the tumor grew to 100 mm^3. In this experiment, the drugs used were divided into 8 groups (n = 6): control; 5-fluorouracil (12.5 mg/kg) (HY-90006, MedChemExpress, USA); naringenin (10 mg/kg) (W530098, Sigma–Aldrich, USA); naringenin (20 mg/kg); naringenin (40 mg/kg); naringenin (10 mg/kg)+5-fluorouracil (12.5 mg/kg); naringenin (20 mg/kg)+5-fluorouracil (12.5 mg/kg); and naringenin (40 mg/kg)+5-fluorouracil (12.5 mg/kg). When the volume of the control group reached 1000–1200 mm^3, the mice were sacrificed, and the tumor mass was removed. Moreover, different kits (CK-MB, Tn-I, AST and ALT) were used to detect the toxicity of different drug treatments to mouse heart and liver tissues.

In addition, for the AOM/DSS-induced orthotopic CRC model, the drug treatments were divided into 6 groups (n = 15): mice in the normal group were administered saline by gavage, and the CRC model group was treated with AOM/DSS without drug administration, naringenin (40 mg/kg), 5-fluorouracil (12.5 mg/kg) (Rani et al., 2021), naringenin (40 mg/kg) combined with 5-fluorouracil (12.5 mg/kg), and Compound c (20 mg/kg) (Abdulrahman et al., 2014) once daily for 11 weeks. According to the nude mouse tumor-bearing experiment, the subsequent dose of naringenin (40 mg/kg) was used in this study.

Cell viability assay

LoVo cells in the logarithmic growth phase were used, and the cell density was adjusted to 5×10^4 cells/ml. Naringenin was added for 24, 48, and 72 h, and 5-fluorouracil was added to each group in 6 wells. After an incubation for 48 h, 20 μl of CCK-8 reagent was added to each well, and the plates were incubated at 37 °C for 4 h.

Evaluation of the effects of drug combinations

The study investigated the drug–drug interaction between naringenin and 5-fluorouracil using the Chou–Talalay method (Chou, 2010). The combination index (CI) was calculated through the CompuSyn software, where CI < 1 is synergistic, CI= 1 is additive and CI > 1 is antagonistic. . The software generated Fa–CI plots to display the effect–combination index curves. Fa represents the drug action effect. Naringenin and 5-fluorouracil were coadministered at different concentrations, with naringenin at 2.5, 5, 10, 20, 40, and 80 μm μmol/L and 5-fluorouracil at 10, 20, 40, 80, 160, and 320 μm μmol/L, all at a fixed ratio of 1:4. Proliferation inhibition was assessed for each group using a CCK-8 kit. Based on the above combined experiments to determine the drug dosage, we divided the LoVo cell experiment into 5 groups for subsequent experiments: Control; naringenin (80 μm μmol/L); 5-fluorouracil (20 μm μmol/L), naringenin combined with 5-fluorouracil, and Compound c (5 μm μmol/L) groups. Among them, Compound c is an AMPK inhibitor.

Transwell assay of the cell migration capacity

The cell concentration was modified to 2×10^5 cells/ml, followed by setting them aside. Each group of cells was incubated individually for a period of 48 h. After that, the transwell chambers were removed, and the medium in the upper chamber underwent two rounds of washing with PBS. Cells that did not migrate were eradicated from the upper chamber using a fresh cotton ball. Next, the cells were fixed with a 70 % ice-ethanol solution for 1h. A 0.5 % crystal violet staining solution was applied to the cells at room temperature for 20 min, followed by rinsing with PBS.

Transwell assay of the cellular invasive capacity

Matrigel was diluted to a final concentration of 1 mg/ml; 100 μl of diluted Matrigel gel was added vertically to the center of the bottom of the upper chamber in the transwell and incubated at 37°C for 4 to 5h to allow the Matrigel was dry to a gelatinous consistency. The invasion cell detection assay was performed as in the migration assay above.

Flow cytometry staining and analysis

Cells were plated in 6-well dishes at a density of 3×10^5 cells per well and exposed to naringenin, 5-fluorouracil, naringenin combined with 5-fluorouracil, and Compound c. Following 48 h of treatment, the cells were collected and stained with Annexin V-FITC and propidium iodide (PI) in accordance with the manufacturer's guidelines (BD Biosciences, San Diego, CA, USA). The levels of ROS and JC-1, were analyzed using flow cytometry (FACS Canto II, BD Biosciences, USA).

Nuclear staining assay

Cell death was evaluated by performing nuclear staining. LoVo cells in the logarithmic growth stage were counted after trypsin digestion, diluted with culture medium to a cell density of 1×10^6 cells/mL, and spread in 24-well plates. After the cells were plated and grown to 85 % confluence in each well, drug interventions were applied for 48 h. Apoptosis was detected in adherent cells by staining treated cells with Hoechst 33342 (ready-to-use) at 37 °C for 30 minutes.

Measurement of mitochondrial and intracellular ROS levels

LoVo cells in the control group and treated with different drugs for 48 h were stained with the MitoSOX Red Mitochondrial Superoxide Indicator fluorescent probe, observed and imaged under fluorescence microscope. The effect on intracytoplasmic ROS levels in LoVo cells was detected by DCFH-DA fluorescent probe.

Measurement of mitochondrial membrane potential

A JC-1 Mitochondrial Membrane Potential Measurement Kit was used to detect the mitochondrial membrane potential (ΔΨm). Briefly, LoVo cells (1×10^6) in the logarithmic growth stage were treated with JC-1 staining working solution after 48 h of drug intervention and washed twice with JC-1 staining buffer (1 ×). Then, 2 mL of fresh cell culture medium was added and cells were placed under a fluorescence microscope; a multifunctional enzyme marker was used to observe and detect the level of JC-1.

Magnetic resonance imaging of tumor formation in mice

In this study, we applied Anker ASM-015 permanent magnetic resonance imaging with a magnetic field strength of 0.15 T using a spin–echo pulse sequence (SE), different scan parameters, echo times (TEs), and pulse repetition times (TRs), and obtained T1-weighted images (T1W1), TR 500 ms/TE 30 ms, and T2-weighted images (T2W1), TR 3000 ms/TE 120 ms, in a cross-sectional plane; depending on the lesion site, sagittal and coronal planes were also selected to facilitate the detection of lesions.

Histological staining

Colorectal and CRC tissues were fixed overnight in 4 % paraformaldehyde (pH 7.4) for histological analysis, embedded in paraffin with corresponding labels, and serially sectioned at 4 μm. Standard hematoxylin and eosin staining was performed. All images of histological staining were captured using a microscope.

Transmission electron microscopy

The excised colorectal tissues were fixed under an electron microscope at room temperature for 2–4 h. After washes with 0.1 M phosphate buffer (pH 7.4), the tissues were fixed in 1 % osmium acid–0.1 M phosphate buffer (pH 7.4) at room temperature (20 °C) for 2 h. The mouse colorectal tissue sections were observed under a transmission electron microscope, and images were acquired for analysis.

Western blot

Total CRC tissue proteins were extracted by grinding mouse CRC tissues homogeneously in sterile centrifuge tubes and adding RIPA lysis buffer supplemented with protease and phosphatase inhibitors. The antibodies and dilution information for the antibodies can be found in Table S4. All the uncropped gel images can be found in Fig. S5 and Fig. S6.

Molecular docking verification

The naringenin SDF format file was downloaded from the PubChem database. We selected the crystal structure of the AMPKα target, downloaded it from the RCSB (RCSB PDB) database, and performed molecular docking through SwissDock. PyMOL was used for visualization.

Statistical analysis

GraphPad Prism 8.0 was used for statistical analysis...When comparing more than two groups, one-way ANOVA or two-way ANOVA was employed. For comparisons of the two groups, unpaired t-test with a two-tailed distribution were used. Data are shown as mean±standard error of the mean (SEM). All experiments were independently repeated at least 3 times with similar time courses and outcomes, and the BALB/c mouse model was established as a one-time experimental outcome with a sufficient number of animals, as indicated in the Fig. legends.

Replications of all experiments are described in the corresponding Fig. legends. $P < 0.05$ (*) and $P < 0.01$ (**) (under multiple hypothesis correction) were considered to indicate statistical significance.

Results

Inhibitory effects of naringenin on the proliferation and invasion of CRC cells

By investigating the inhibitory effect of naringenin on CRC proliferation, we found that different concentrations of naringenin inhibited the proliferation of LoVo cells to varying degrees in a concentration-time-dependent manner ($P < 0.05$) (Fig. 1A). The inhibition of cell proliferation was significantly greater after 48 h of naringenin treatment than after 24 h ($P < 0.05$). Therefore, subsequent experiments identified 48 h as the optimal time of administration (Table S1). The inhibition of proliferation by 5-fluorouracil at 48 h also increased significantly with increasing concentrations (Fig. 1B, Table S2). The IC_{50} at 48 h was 329.30 μm μmol/L for naringenin and 87.61 μm μmol/L for 5-fluorouracil. The Chou–Talalay method was used to calculate the CI. The data showed that there was a notably higher inhibition rate of proliferation observed when naringenin and 5-fluorouracil were used in combination compared to when either compound was used alone. The combination treatment displayed a synergistic effect on CRC cells, with a CI value of less than 1 at every concentration tested (refer to Fig. 1C, D, and Table S3). Additionally, we investigated the impact of naringenin on the migration and invasion of CRC cells. Results from the Transwell invasion assay demonstrated that treatments with naringenin, 5-fluorouracil, or the combination of both significantly decreased the number of invading cells compared to the control group ($P < 0.01$) (see Fig. S1 and Fig. S2).

Naringenin inhibits colorectal carcinogenesis associated with colitis

Previous cell-based experiments have shown that naringenin can inhibit the proliferation of CRC cells. Subsequently, the effect of naringenin on tumor growth was further investigated through in vivo animal experiments (Fig. 2A). After 28 days of the experiment, the animals were sacrificed, and the subcutaneous tumors were removed and weighed. The results indicated that, compared to those in the control group, the volume and weight of subcutaneous tumors in mice decreased significantly after treatment with increasing naringenin concentrations, leading to a notable increase in the tumor inhibition rate (Fig. 2B-E). The histological analysis of HE staining revealed (Fig. 2F, I) that low, medium, and high doses of naringenin alone had no significant impact on the tissue morphology of the heart, liver, spleen, lung, or kidney, but naringenin combined with 5-fluorouracil reduced the degree of necrosis and myocardial atrophy compared with the group that was treated with 5-fluorouracil alone, and these effects gradually recovered with the increase in the dose of the combined treatment. As the dose increased, the degree of liver damage decreased, but the liver damage did not completely recover or even disappear. No morphological changes or damage to the spleen tissue were observed in any of the groups. In the lung tissue of the 5-fluorouracil group, the alveolar spaces were not clean, causing pulmonary hemorrhage and pulmonary edema. As the dose of naringenin increased, the lumen of the renal tubules gradually

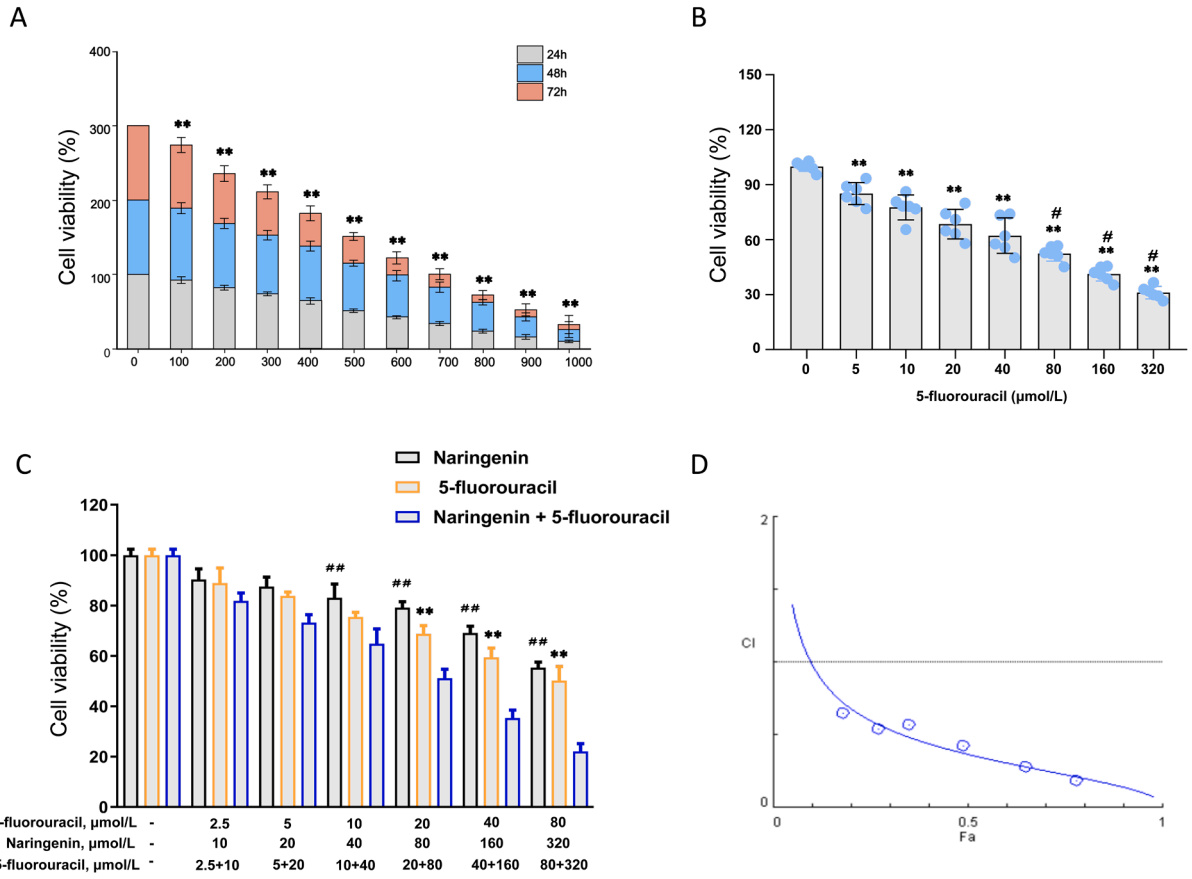

Fig. 1. Inhibitory effect of naringenin and 5-fluorouracil on the proliferation of CRC cells. (A) Inhibition of LoVo cell proliferation by naringenin, compared with the control group, $^{**}P < 0.01$. (B) Inhibition of LoVo cell proliferation by 5-fluorouracil, compared with the control group, $^{**}P < 0.01$; compared with the previous concentration group, $^{\#}P < 0.05$. (C) Effect of naringenin combined with 5-fluorouracil on LoVo proliferation. $^{\#}P < 0.05$ and $^{\#\#}P < 0.01$ for the comparison of the combination group with the naringenin group; $^{*}P < 0.05$ and $^{**}P < 0.01$ for the comparison of the combination group with the 5-fluorouracil group. (D) Effect of naringenin combined with 5-fluorouracil on LoVo cells according to the combination index curve. Source data are provided as a Source Data file.

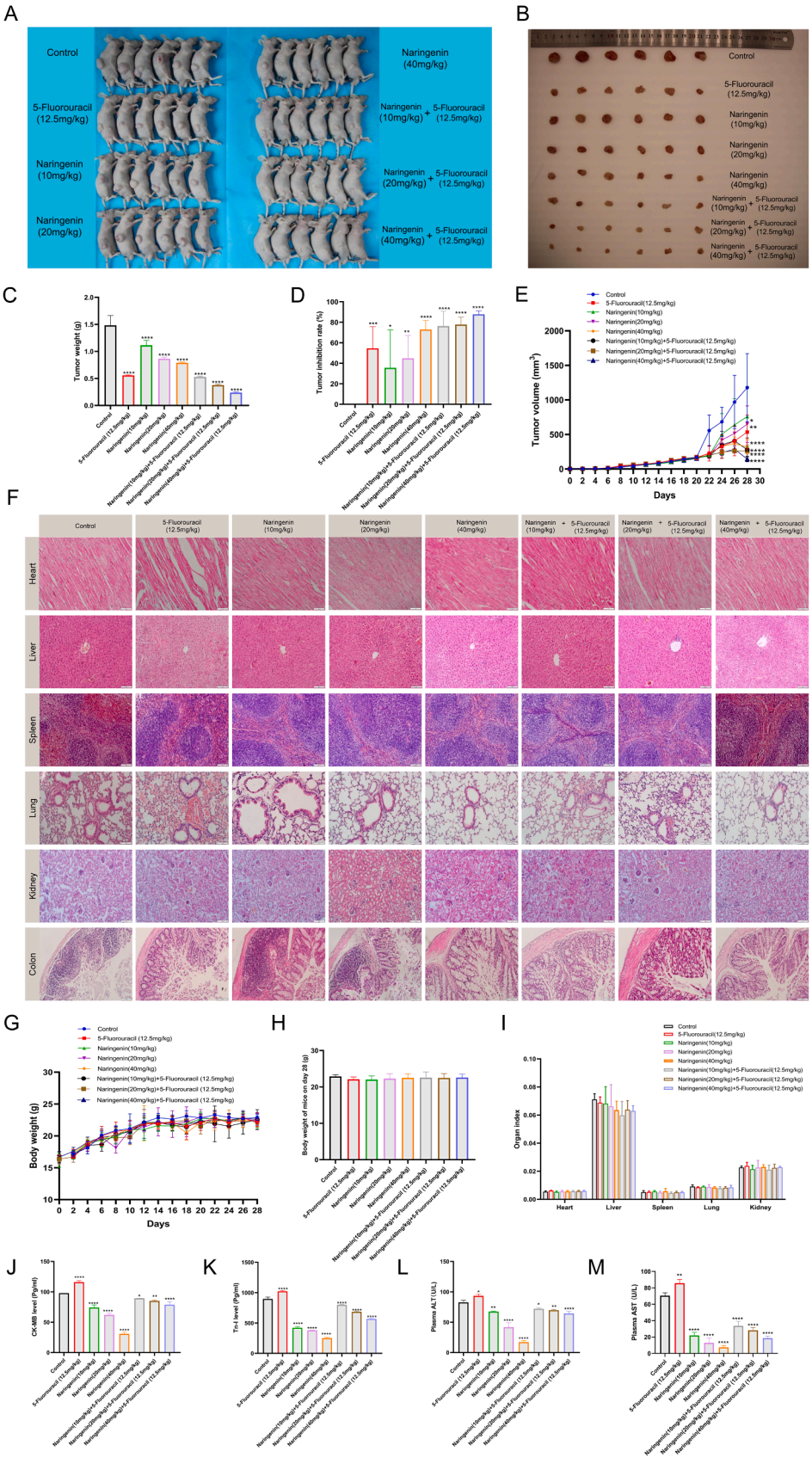

(caption on next page)

Fig. 2. Effect of naringenin on subcutaneous tumor formation in male BALB/c-nu mice. (A) Representative images of subcutaneous tumors in male BALB/c-nu mice from different drug treatment groups. (B) Images of tumors removed from 8 groups of mice treated with different concentrations of drugs. (C-E) Statistical analysis revealed that as the concentration of naringenin increased, the volume and weight of subcutaneous tumors in nude mice were significantly decreased, and the combination treatment had the most significant effect. (F) Analysis of HE staining of male BALB/c-nu mice. Scale bar:100 μm. (G-H) Growth and weight of BALB/c-nu mice. (I) Indices of five internal organs (heart, liver, spleen, lungs and kidneys) were measured. (J-K) Analysis of CK-MB activity and Tn-I levels; (L-M) analysis of AST and ALT levels. $^{*}P < 0.05$; $^{**}P < 0.01$, and $^{***}P < 0.001$.

became regular, the contents in the lumen gradually disappeared and were cleared and metabolized, and the kidney structure gradually recovered. However, after treatment with high doses of the combination of the two compounds, the intestinal lumen was clean and translucent, and the intestinal mucosa appeared more complete.

BALB/c-nu mice showed balanced growth and weight, which did not

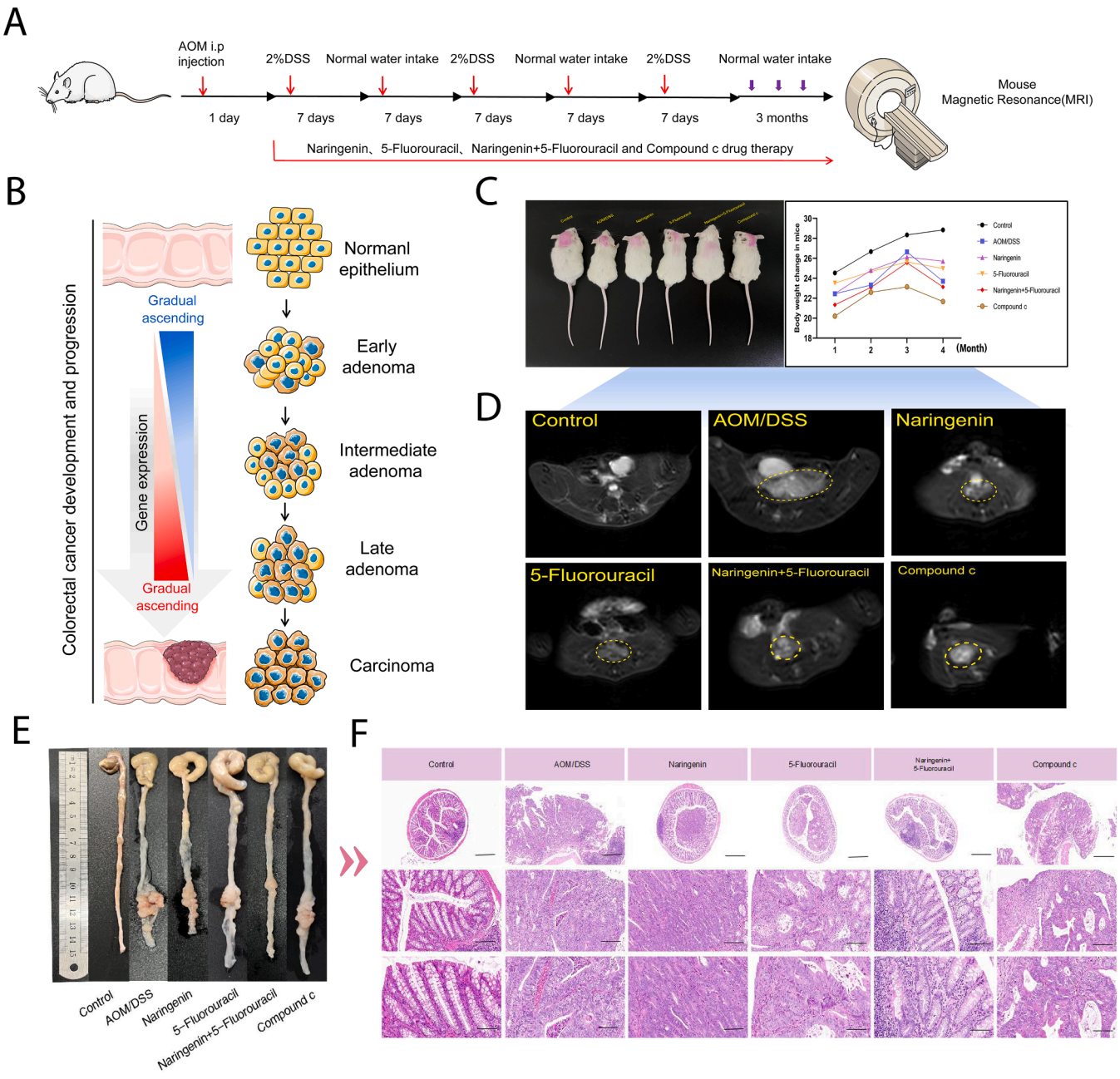

Fig. 3. Naringenin inhibits colon tumor development in the AOM/DSS model. (A) Animal experimental design scheme: the process of establishing AOM/DSS-induced CRC model mice. (B) Schematic diagram of the evolution of CRC (CRC starts from the malignant transformation of colorectal adenomas, and after undergoing hyperproliferation and developing into polyps, the normal epithelium can develop into CRC through early, intermediate and late adenomas and even distant metastases). (C) Apparent morphology (left panel, showing morphological changes at week 12) and weight changes (right panel, starting with the starting weight at week 1 and ending with euthanasia) in mice after treatment with different drugs, n = 15 mice per group. (D) Magnetic resonance imaging of mice (the tumor size is partially circled in yellow; cross-sectional image representation). (E) Gross pathology of colorectal tissues from mice. (F) Histological images of colonic tissue (the first row shows HE staining at 5 × magnification, the middle row shows HE staining at 20 × magnification, and the third row shows HE staining at 40 × magnification). Source data are provided as a Source Data file.

differ significantly between the different drug groups (Fig. 2G, H). The potential of naringenin to alleviate 5-fluorouracil-induced cardiotoxicity was assessed, and higher CK-MB activity and Tn-I levels were detected in the 5-fluorouracil group than in the control group. However, the administration of low, medium, and high doses of naringenin resulted in a significant reduction in CK-MB activity and Tn-I levels compared to those in the control group. Furthermore, combined treatment with 5-fluorouracil and naringenin also led to substantial decreases in CK-MB activity and Tn-I levels, suggesting that naringenin has cardioprotective effects against 5-fluorouracil-induced toxicity (Fig. 2J, K). Additionally, AST and ALT levels were elevated in both the 5-fluorouracil and control groups, indicating potential liver damage from the disease itself and 5-fluorouracil administration. Conversely, the administration of naringenin at low, medium, and high dose group had significantly lower AST and ALT levels compared to the control group (Fig. 2L, M). Overall, based on the effects of the abovementioned doses of the combination treatment on mouse tumors and organs, we found that naringenin (40 mg/kg) combined with 5-fluorouracil (12.5 mg/kg) can reduce the cardiotoxicity and liver damage caused by 5-fluorouracil, and the effect is the most significant.

We considered it more meaningful to use an animal model of inflammatory carcinoma in situ CRC. We constructed an in mouse CRC animal model induced by AOM/DSS to investigate the preventive effect of naringenin on CRC. The workflow used to construct the animal model is shown in Fig. 3A. CRC progresses through a long process, from proliferative polyps to adenoma and then to adenocarcinoma (Siegel et al., 2023b). Its occurrence and development are complex, multifactorial, and multistage processes, and after precancerous lesions, it eventually evolves into CRC (Fig. 3B). Mice in the naringenin alone group and in the naringenin combined with 5-fluorouracil group showed transient weight loss after each course of DSS; however, the weight of the mice in the naringenin group did not differ significantly between the 1st and 2nd months of drug treatment, while the weight of the mice decreased sharply in the 3rd and 4th months (Fig. 3C). We also examined the growth of tumor masses in mice using magnetic resonance imaging (MRI) and found no abnormalities in the intestinal wall of normal mice; adenocarcinoma in the intestine of the model AOM/DSS group caused thickening of the intestinal wall and narrowing of the intestinal canal, and clear wall nodules and soft tissue masses were observed, while naringenin, 5-fluorouracil and naringenin combined with 5-fluorouracil produced smaller intestinal wall nodules on MRI. Smaller masses were more evident in the naringenin combined with 5-fluorouracil group than in the model AOM/DSS group (Fig. 3D), whereas no significant improvement was detected in tumors of the intestinal wall in the mice from the Compound c group. The surface of the intestinal tract morphology was smooth and flat in the blank group. Compared with those of the AOM/DSS group, the intestinal tracts of the other four groups were obviously thickened, with increased surface area and tumor-like tissue formation. In the naringenin group, 5-fluorouracil group and naringenin combined with 5-fluorouracil group, fewer masses, flatter intestinal tracts and more elongated intestinal canals were observed compared with the model AOM/DSS group, indicating that naringenin and 5-fluorouracil had some intervention effect on colorectal inflammatory cancer transformation (Fig. 3E).

HE staining analysis of mouse colorectal tissue (Fig. 3F) showed that the colorectal tissue in the blank group was normal, the mucosal structure was intact, the intestinal villi were normal, and the goblet cells were evenly arranged and distributed. In the AOM/DSS CRC model group, the colorectal mucosa structure was disordered, intestinal villi disappeared, goblet cells were deformed, nuclei were deeply stained, scattered and irregularly distributed, mucosal ulcers formed, and a large number of CRC cells appeared, indicating that the orthotopic tumor model was successful. In the naringenin group, the glands were disordered and infiltrated with numerous inflammatory cancer cells, but the number of cancer cells was reduced in the naringenin group compared to the model group. In the 5-fluorouracil group, the goblet cells were arranged in disorder, and a small number of inflammatory cancer cells were arranged. The naringenin combined with 5-fluorouracil group showed local inflammatory reaction. In contrast, in the Compound c group, the colorectal mucosa structure was disordered, the intestinal villi disappeared, and the goblet cells were deformed, no significant reduction in cancer cells was found. These results indicate that the combination of naringenin and 5-fluorouracil can alleviate the inflammatory cancer cell status in the intestines of mice, delay the progression of CRC, and protect the intestinal mucosa of mice compared with the drugs alone.

Naringenin induces apoptosis in CRC cells

When cells are stimulated by various external factors (e.g., naringenin and 5-fluorouracil), apoptosis-related pathways are activated and cells begin to shrink, resulting in a dense cytoplasm and more compact organelles and chromatin. Subsequently, plasma membrane blistering occurs, which tightly wraps around the ruptured nuclear fragments, leading to the formation of apoptotic vesicles (Fig. 4A). Hoechst 33342 staining revealed that the control group had a uniform cell morphology and moderate fluorescence intensity; the naringenin and 5-fluorouracil groups both exhibited nuclear consolidation, dense staining, an uneven distribution of nuclear chromatin, some crescent shapes, nuclear rupture, distribution along the cell membrane, and the appearance of apoptotic vesicles. In addition, the cells treated with Compound c exhibited less nuclear fragmentation, suggesting that Compound c could attenuate the apoptotic effect of CRC, while the cells treated with naringenin combined with 5-fluorouracil exhibited typical apoptotic karyotype changes, such as partial nuclear fragmentation (Fig. 4B).

Mitochondrial ROS fluorescence was measured to determine the role of naringenin and naringenin combined with 5-fluorouracil in oxidative stress in CRC and the results showed that mitochondrial ROS levels were lower in the blank control group, and intracellular fluorescence gradually increased in the naringenin, 5-fluorouracil and naringenin combined with 5-fluorouracil groups, with a significant increase in the fluorescence density in the naringenin combined with 5-fluorouracil group, indicating that naringenin or 5-fluorouracil could significantly increase the intracellular ROS level in LoVo cells ($P < 0.01$). The increase in ROS levels was more pronounced after the administration of naringenin combined with 5-fluorouracil ($P < 0.01$). The mitochondrial ROS level was significantly attenuated in the Compound c group compared with the naringenin combined with 5-fluorouracil group (Fig. 4C). Subsequent MitoSOX Red staining revealed that naringenin induced changes in superoxide levels in CRC cell mitochondria. The intensity of red fluorescence detected in the naringenin combined with 5-fluorouracil group was greater than that in the control group (Fig. 4D), indicating that naringenin combined with 5-fluorouracil could increase superoxide levels in the mitochondria of CRC cells.

The mitochondrial membrane potential ($\Delta\Psi m$) results indicated that LoVo cells in the blank control group exhibited strong red fluorescence after JC-1 staining, suggesting that the vast majority of cancer cells had normal mitochondrial function. In the naringenin-, 5-fluorouracil-, and naringenin combined with 5-fluorouracil-treated groups, JC-1 staining significantly enhanced intracellular green fluorescence ($P < 0.01$), while naringenin combined with 5-fluorouracil was more effective than either treatment alone ($P < 0.05$). In addition, further treatment with Compound c resulted in a significant increase in red fluorescence ($P < 0.001$) according to JC-1 staining (Fig. 4E), and the increase in the cellular $\Delta\Psi m$ reversed the increase in red fluorescence. These results indicate that naringenin or 5-fluorouracil can decrease the mitochondrial membrane potential in LoVo cells, resulting in mitochondrial dysfunction and eventually apoptosis.

In addition, we analyzed the effects of naringenin alone or in combination with 5-fluorouracil on LoVo cell apoptosis using flow cytometry to investigate the synergistic inhibition of CRC LoVo cell growth by

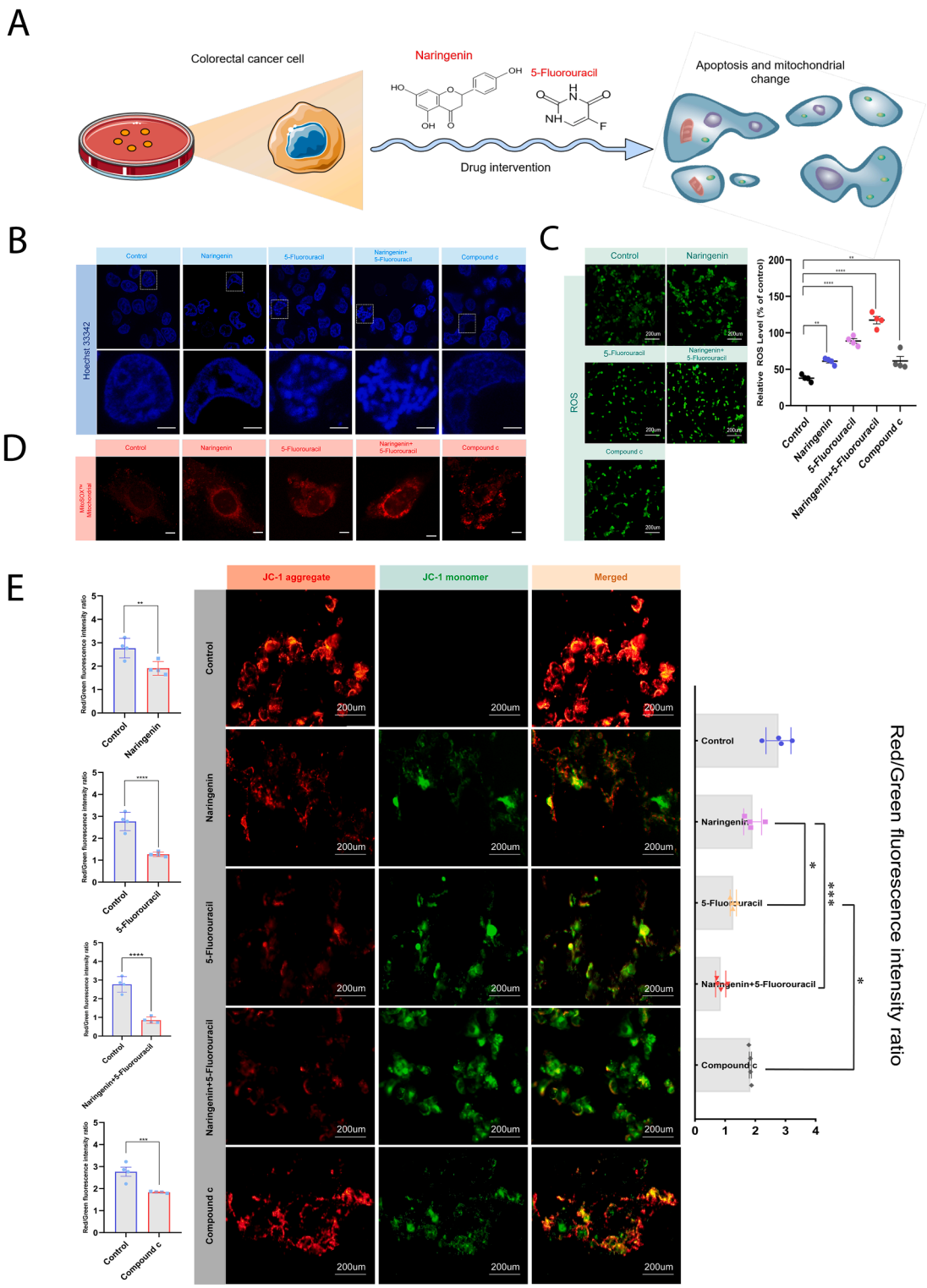

Fig. 4. CRC cells undergo apoptosis after treatment with different drugs. (A) Schematic diagram of the mitochondrial and apoptotic changes occurring in CRC LoVo cells after intervention with naringenin and naringenin combined with 5-fluorouracil in this study. (B) Apoptosis of each group of cells was detected after Hoechst 33342 staining. Scale bar: 200 μm. (C) Oxidative stress and mitochondrial dysfunction induced by naringenin and naringenin combined with 5-fluorouracil in CRC cells. After pretreatment with naringenin (80μmol/L), 5-fluorouracil (20μmol/L), the combination of drugs and Compound c (5μmol/L) for 48 h, the intracellular ROS levels were detected in CRC LoVo cells using the probe DCFH-DA; the control group was treated with culture medium only. Scale bar: 200 μm. (D) Fluorescence microscopy combined with MitoSOX staining was used to observe the superoxide content in the mitochondria of CRC LoVo cells without drug intervention. Scale bar: 100 μm. (E) The JC-1 probe was used to detect changes in the mitochondrial membrane potential and the ratio of JC-1 monomers/aggregates in CRC LoVo cells after drug treatment. All experiments were performed at least three times. The data are presented as the means ± standard deviations (means ± SDs). A t test was used for the statistical analysis of two groups, one-way ANOVA was used to compare data between multiple groups, and GraphPad Prism 8.0 was used for graphing. The asterisk (*) is used to represent a comparative statistically significant result. $^{*}P < 0.05$, $^{**}P < 0.01$, and $^{***}P < 0.001$. Source data are provided as a Source Data file. DCFH-DA: dichlorodihydrofluorescein diacetate; ROS: reactive oxygen species.

naringenin and 5-fluorouracil. After 48 h, JC-1 labeling revealed enhanced green fluorescence in cells treated with naringenin, 5-fluorouracil, and Compound c, indicating a significant increase in the monomeric form JC-1 indicating the membrane potential and a decrease in the mitochondrial membrane potential, with the naringenin and 5-fluorouracil combination group showing the most pronounced effect (Fig. 5A). Furthermore, ROS levels in LoVo cells increased after treatment with naringenin, 5-fluorouracil, and Compound c, with the combination of naringenin and 5-fluorouracil producing the greatest increase (Fig. 5B). The flow cytometry results were consistent with the results in the fluorescence plot.

Naringenin can promote mitochondrial fusion in mice with AOM/DSS-induced CRC

We analyzed the mitochondrial ultrastructure of colorectal epithelial

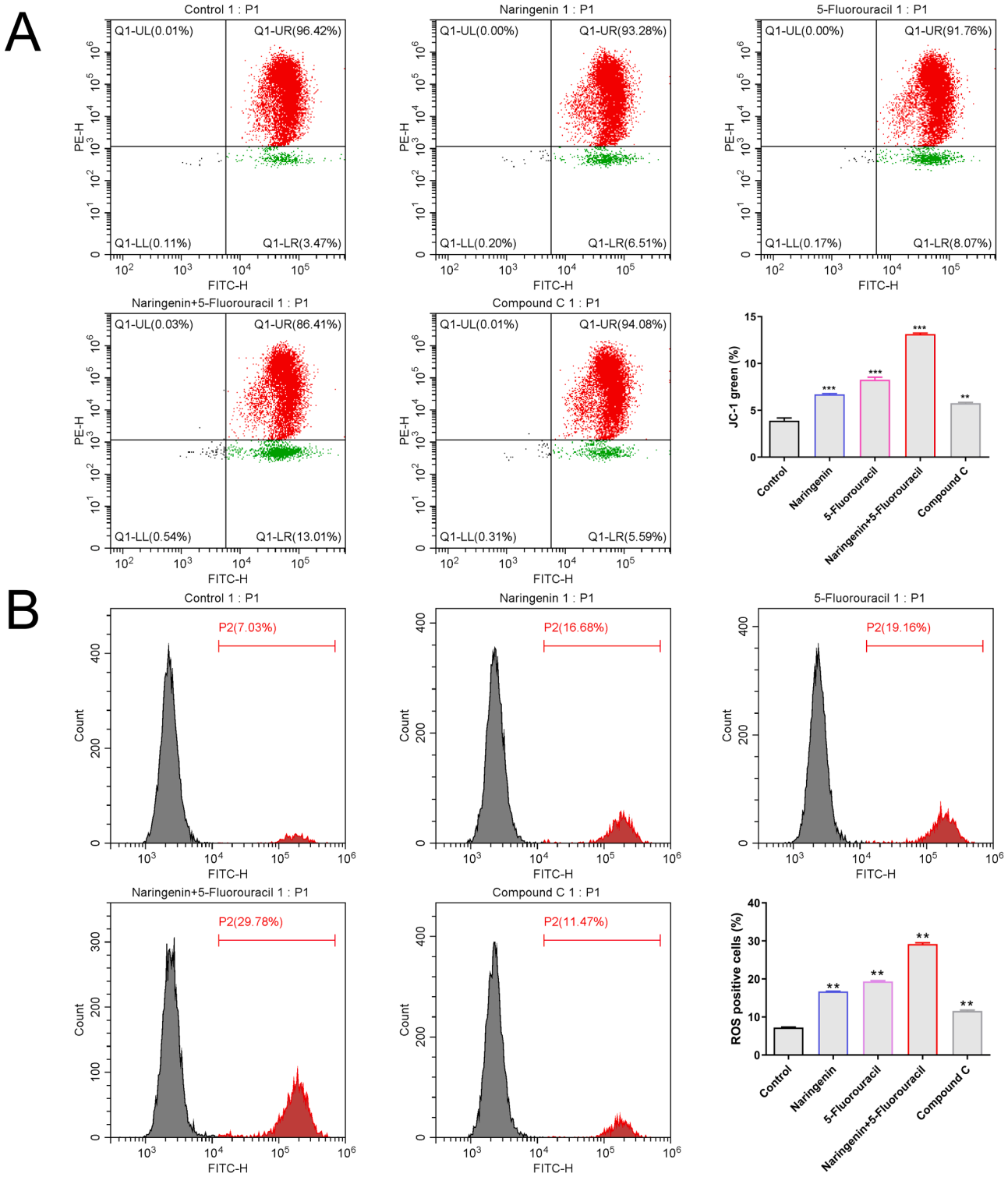

Fig. 5. Naringenin induces apoptosis in CRC cells through ROS generation and mitochondrial dysfunction. (A) Analysis of theMM P (JC-1) and (B) ROS levels using flow cytometry. *$P < 0.05$, **$P < 0.01$, and ***$P < 0.001$.

cells to examine the effect of naringenin on tumor cell ultrastructure (Fig. 6A). Changes in mitochondrial morphology at colorectal tumor sites in mice were detected, as shown in Fig. 6B. The mitochondrial structure of colorectal cells in the normal group was intact, with a uniform distribution of chromatin in the nucleus and a long rod shape. In the AOM/DSS model group, the mitochondrial structure was disrupted, mitochondrial fission was significantly increased, and mitochondria were significantly shorter and rounder. density of the mitochondrial matrix distribution was relatively greater in the naringenin, 5-fluorouracil and naringenin combined with 5-fluorouracil groups than in the AOM/DSS group. Compared with those in the AOM/DSS group, mitochondrial fission was significantly reduced and the mitochondrial length was significantly increased in the colorectal tumors of the mice after intervention with naringenin or 5-fluorouracil alone or naringenin combined with 5-fluorouracil. In contrast, after further activation of AMPK in addition to the Compound c receptor in the naringenin combined with 5-fluorouracil group, mitochondrial fission in the colorectal tumors of the mice was significantly increased, and the mitochondria were shorter. We used laser confocal microscopy with MitoTracker Red staining to compare the changes in mitochondrial morphology more objectively and found that the lengths of mitochondria in the naringenin, 5-fluorouracil and naringenin combined with 5-fluorouracil groups were significantly longer than that in the control group (Fig. 4D). These results suggested that naringenin and naringenin combined with 5-fluorouracil might lead to the dysregulation of mitochondrial dynamics with reduced division and increased fusion.

Naringenin upregulates AMPK in CRC cells to promote mitochondrial fusion and induce apoptosis

Next, we explored the mechanistic effects of naringenin on cancer cells using protein blotting (Fig. 7A). The Western blot results blot results showed that naringenin and 5-fluorouracil treatment of LoVo cells increased p-AMPK protein expression, while the protein levels of p-mTOR and p-p70S6k decreased, but no significant differences in the levels of the AMPK, mTOR and p70S6k proteins were observed. Compared with the single-drug group, the naringenin combined with 5-fluorouracil group exhibited significantly increased p-AMPK levels and decreased p-mTOR and p-P70S6K levels. Levels of p-AMPK were decreased and levels of the p-mTOR and p-P70S6K proteins were increased in the Compound c group compared with the naringenin and 5-fluorouracil combination group. These results suggested that the combination of naringenin and 5-fluorouracil activated AMPK and inhibited the mTOR and p70S6k pathways in LoVo cells (Fig. S3).

We treated LoVo cells with Compound c to verify whether naringenin regulates mitochondrial dynamics in CRC cells through the AMPK pathway. Compared with the control group, naringenin and 5-fluorouracil interventions significantly reduced KIF5B, Miro1 and DRP1 levels ($P < 0.05$) and increased the levels of the MFN2 and Cyt-c proteins ($P < 0.05$) in LoVo cells after the naringenin and 5-fluorouracil intervention, and the effect of naringenin combined with 5-fluorouracil was more significant (Fig. 7B, C). In contrast, the Cyt-c level was significantly reduced ($P < 0.01$) and the level of the mitochondrial fission protein DRP1 was significantly increased ($P < 0.01$) in the Compound c group compared with the naringenin and 5-fluorouracil combination group. This finding suggests that naringenin combined with 5-fluorouracil can inhibit colorectal cancer growth by inhibiting Miro1, a mitochondrial bridging protein, and Drp1, a mitochondrial division protein, and promoting the expression of Mfn2 and Cyt-C, mitochondrial fusion proteins, as well as down-regulating the kinesin of KIF5B, which increases the fusion/decreases the division of mitochondria, thus increasing the level of AMPK.

Naringenin and 5-fluorouracil considerably increased Caspase-9, Caspase-3, and Bak protein levels compared to the control group (*P*

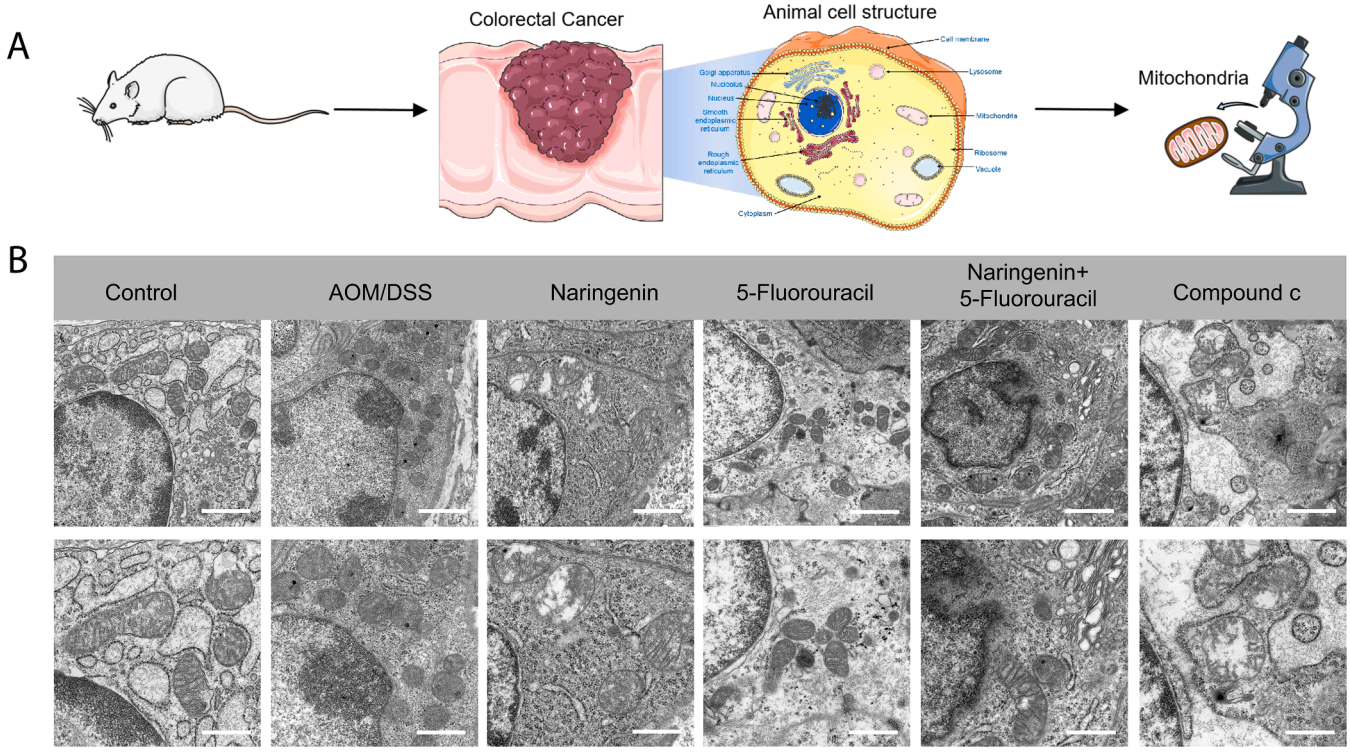

Fig. 6. Naringenin improves the mitochondrial structure. (A) Schematic diagram of the observed colorectal ultrastructure in mice. (B) Mitochondrial ultrastructure in colorectal epithelial cells observed using transmission electron microscopy (magnification, × 10.00k). The number and structure of mitochondria in colorectal mucosal cells from the control group were normal. The mitochondrial structure in the AOM/DSS group was impaired. Mitochondria and nuclei appeared to be altered to different degrees after treatment with naringenin, 5-fluorouracil or naringenin combined with 5-fluorouracil. Naringenin combined with 5-fluorouracil treatment ameliorated AOM/DSS-induced damage to the mitochondrial structure in colorectal epithelial cells.

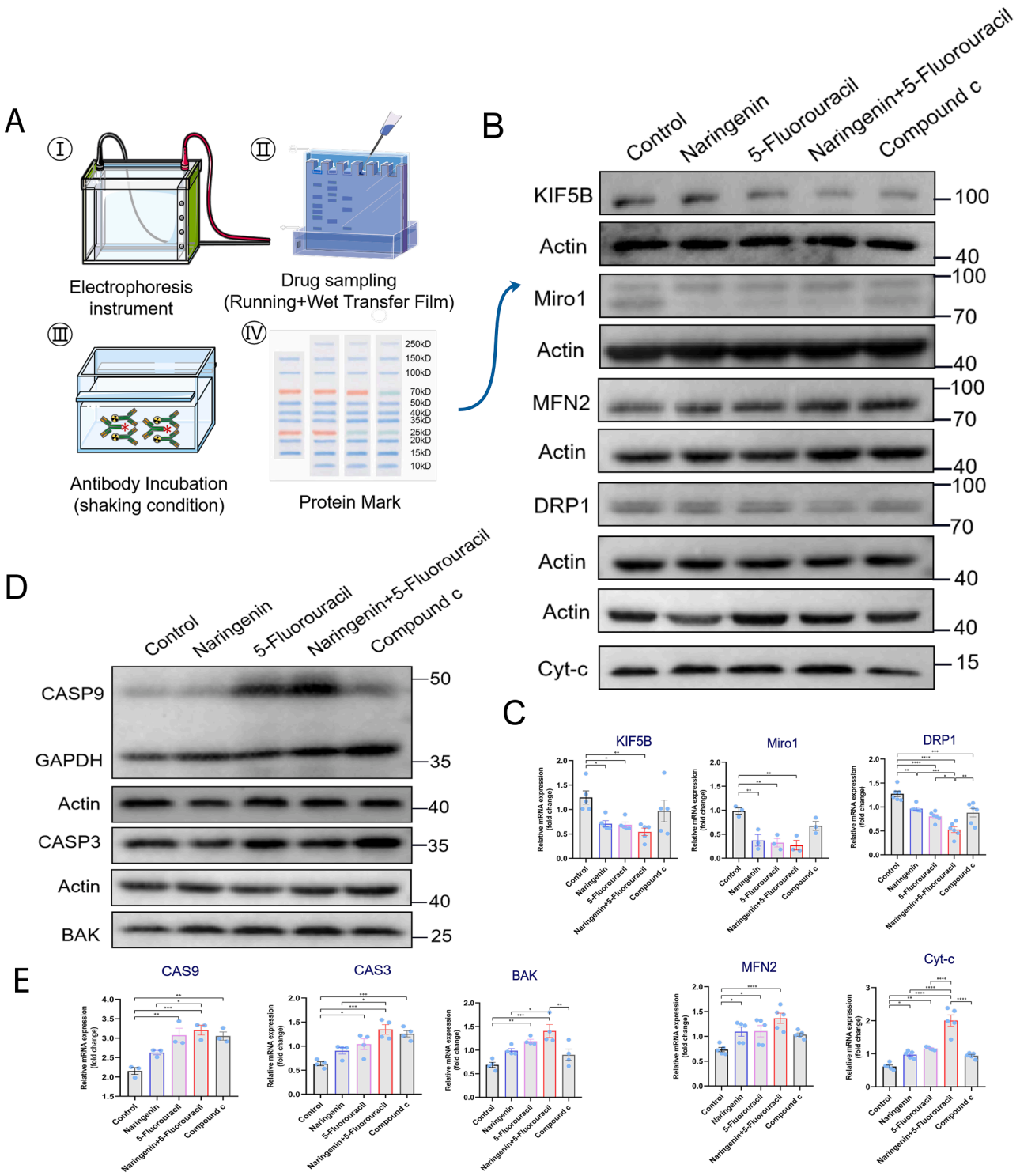

Fig. 7. Naringenin and naringenin combined with 5-fluorouracil inhibit the expression of proliferation-related genes in CRC LoVo cells. (A) The presence of reactive antibodies against Bio-Rad protein markers in CRC LoVo cells. The marker proteins were separated on 10 % SDS−PAGE gels, and the samples were sequentially loaded. For visualization, a colored protein marker was added to the lane at the edge of the gel with lysates from the drug-treated cells for the protein blot analysis. (B) After treating LoVo cells with different drugs for 48 h, the effects of naringenin on KIF5B, Miro1, MFN2, DRP1 and Cyt-c mitochondrial function were detected by performing a protein blot analysis. (C) Statistically significant p values were observed for naringenin, 5-fluorouracil and naringenin combined with 5-fluorouracil compared to the control group; the data represent three independent experiments. (D) The effects of different drugs on the expression of the apoptotic proteins CASP9, CASP3 and BAK were detected by protein blotting. (E) Levels of apoptosis-related proteins were significantly different, and the data represent three independent experiments. The data in C and E are presented as the means±SEMs; one-way ANOVA was used for the analysis. Source data are provided as a Source Data file.

<0.05) (Fig. 7D and E). The combined effect of naringenin and 5-fluorouracil was more pronounced than when used individually ($P<0.01$). Compound c notably decreased Bak protein levels compared to the combination of naringenin and 5-fluorouracil ($P<0.01$). Furthermore, Bax and cleaved caspase-3 expression was significantly up-regulated and Bcl-2 expression was down-regulated in the LoVo cell co-treatment group compared with the control or single drug group ($P<0.05$) (Fig. S4). Expression levels of Bax, cleaved caspase-3, Caspase-9, Caspase-3 and Bak were significantly up-regulated and Bcl-2 was down-regulated ($P<0.05$) in the LoVo cell co-treatment group. These results indicate that the combined use of naringenin and 5-fluorouracil synergistically hinders the growth of CRC LoVo cells and is linked to enhanced activation of apoptotic pathways.

Naringenin promotes mitochondrial fusion and apoptosis in CRC cells in vivo by activating AMPK

The in vitro results showed that naringenin combined with 5-

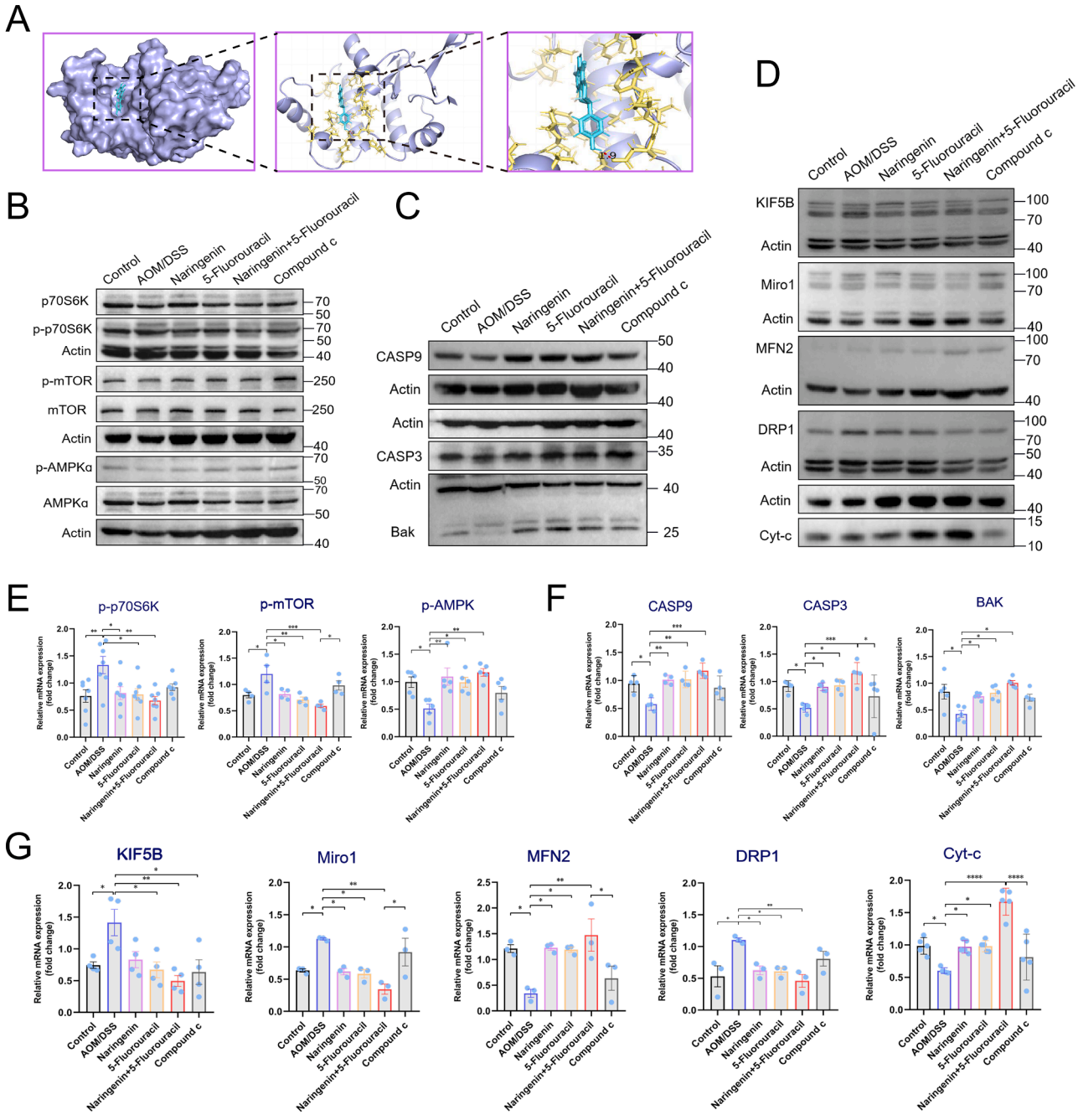

Fig. 8. Molecular mechanisms affecting the AMPK signaling pathway, mitochondrial function and apoptosis pathway-related proteins in the AOM/DSS model. (A) Molecular docking of naringenin and the core target AMPK. (B) Detection of the expression levels the AMPK signaling pathway-related proteins AMPKa, mTOR and p70S6K. (C) Expression of the apoptosis-related proteins CASP9, CASP3 and BAK in CRC tissues. (D) Expression levels of the mitochondria-associated proteins KIF5B, Miro1, MFN2, DRP1 and Cyt-c. The values under each lane indicate the relative density of the band normalized to that of β-actin. (E) AMPK phosphorylation and protein ratio statistical graph. (F) Apoptosis-related protein ratio statistical graph. (G) Statistical graph of mitochondria-related protein ratios. The data are presented as the means ± SEMs of at least three independent experiments. Statistical significance: $^{**}P < 0.01$ and $^{***}P < 0.001$ compared with the AOM/DSS-treated group. Abbreviations: AOM/DSS, azoxymethane/dextran sodium sulfate. Source data are provided as a Source Data file.

fluorouracil activated AMPK and regulated mitochondrial dynamics, resulting in the apoptosis of LoVo cells. Furthermore, the results were validated in vivo by examining colorectal tissue samples extracted from the AOM/DSS model using Western blotting (Fig. 8), and compared with the control group, the expression levels of p-AMPK, MFN2, Cyt-C, Caspase-9, Caspase-3, and Bak proteins were significantly lower in the tissues of the AOM/DSS CRC group in the in situ mouse CRC animal model ($P < 0.05$), while the expression levels of mTOR, p-p70S6K, KIF5B, Miro1, and DRP1 were significantly higher in the tissues of the AOM/DSS CRC group ($P < 0.05$). and DRP1 proteins were significantly increased. Overall, our in vivo results were consistent with the in vitro findings. In addition, we used SwissDock for molecular docking simulations and found that the docking energy of naringenin and AMPKα was -6.731 kcal/mol, indicating a significant interaction with AMPKα (Fig. 8A). Thus, these data suggest that naringenin promotes apoptosis in CRC cells through the activation of AMPK signaling pathway to mediate mitochondrial dynamics.

Discussion

Based on colonoscopy screening and treatment advances, accompanied by lower CRC incidence and mortality rates in some highly developed countries, an increasing trend of incidence and mortality is still observed in a number of developing countries (Kaczanowski, 2016). Therefore, the development of novel treatment strategies or therapeutic agents for CRC are urgently needed to achieve clinical benefits. Although natural flavonoids hold new promise for the treatment and prevention of CRC, the antitumor effects of natural flavonoids on CRC and their underlying mechanisms have not been fully revealed. This study shows for the first time the anticancer mechanism by which naringenin synergizes with 5-fluorouracil in CRC cells. Due to the current therapeutic dilemma of treating CRC, the combination of naringenin and 5-fluorouracil may become an emerging therapeutic approach. An increasing number of investigations have focused on the biosafety and long-term use of natural small-molecule extracts, as well as on treatments targeting multiple pathways and elucidating the molecular mechanisms underlying their activity (Fan et al., 2023; Maphetu et al., 2022; Yang et al., 2022).

Accumulating studies have documented the increased efficacy of natural drugs in combination with certain therapeutic agents. Typical examples include curcumin (Firouzi Amoodizaj et al., 2020), resveratrol (Gupta et al., 2023), and bitter ginseng alkaloids (Hu et al., 2021a). The activation of the naringenin core gene interstitial epidermal transforming factor (MET) can induce the invasion and metastasis of CRC cells (Wang et al., 2020). Moreover, METalso participates in the immune escape of CRC cells. Naringenin may inhibit the metastasis of CRC and improve the prognosis of patients by acting on the MET gene. Studies have shown that 6-C-(E-phenylvinyl)-naringenin effectively inhibits tumor growth in CRC xenograft models by inhibiting cyclooxygenase-1, without significant systemic toxicity (Li et al., 2014). However, no published reports have revealed the effects and mechanisms of naringenin and 5-fluorouracil in combination for CRC treatment.

Previous research conducted by our team has demonstrated that metformin has the ability to directly impede CRC cell growth, tumor blood vessel formation, and spread by stimulating AMPK within the LKB1-AMPK-AKT signaling pathway (Chen et al., 2019). Additionally, it can induce programmed cell death in colorectal cells. Similar to metformin, naringenin exhibits comparable effects and can trigger the AMPK pathway. This compound is capable of suppressing the production of new glucose, combating diabetes, reducing inflammation, and restraining cell growth by enhancing AMPK activity. These results suggest that activating AMPK may become a promising therapeutic target for the treatment of CRC. Nevertheless, the synergistic impact and underlying mechanism of naringenin and 5-fluorouracil in activating the AMPK signaling pathway to modulate mitochondrial function in CRC have not been documented in the existing literature, necessitating further experimental validation. In this study, we observed that naringenin has an inhibitory effect on the proliferation of human CRC LoVo cells.

Naringenin, in combined with 5-fluorouracil, exhibited dose- and time-dependent inhibition of LoVo CRC cell growth. While naringenin alone had limited effects on CRC cell proliferation, it demonstrated synergistic impacts when combined with 5-fluorouracil. Therefore, there is a suggestion that naringenin combined with 5-fluorouracil to elicit an anticancer response in CRC therapy. Previous research has indicated that naringenin triggers apoptosis in breast (Zhao et al., 2024), lung (Memariani et al., 2021), and gastric cancer cells (Zhang et al., 2021). Our investigation confirmed the pro-apoptotic effects of naringenin on CRC cells and also unveiled that the combined treatment of naringenin and 5-fluorouracil significantly intensified apoptosis compared to individual drug regimens. Moreover, naringenin was observed to impede cancer cell invasion and metastasis in several studies (Gumushan Aktas and Akgun, 2018; Lian et al., 2021; Shi et al., 2021). Our findings indicate that the combined administration of naringenin and 5-fluorouracil synergistically inhibits the proliferation of LoVo CRC cells, with a more pronounced effect compared to single-drug therapies. This may be attributed to its capacity to inhibit the growth of human CRC cells by activating AMPK and suppressing the mTOR and subsequent p70S6K signaling pathways.

The intestinal epithelium is the most dynamic tissue in the body because it is constantly renewed. Disturbances in the balance between proliferation, differentiation and apoptosis may lead to the development of CRC. CCRC is initiated by DNA damage. The close association between intestinal inflammation and CRC is well-documented. In adult jejunum, AMPK mainly localizes in the apical part of the villous epithelium (Ma et al., 2024). DSS induced colitis is exacerbated in AMPK Vil-Cre KO mice (Olivier et al., 2022), whereas metformin administration lessens colitis in interleukin-10-deficient mice (Liu et al., 2024) and mice with DSS-induced colitis (Wang et al., 2022). AMPK's potential to suppress intestinal tumorigenesis by alleviating inflammation is worthy of attention. Recent insights on AMPK's role in cancer reveal its multifaceted nature, with evidence suggesting its ability to either suppress or promote tumor growth, depending on tumor type and context (Zadra et al., 2015). Activation of AMPK phosphorylation by natural chemosynthetic drugs has been found to inhibit cancer cell growth (Li et al., 2023), implying AMPK's tumor-suppressive potential in specific scenarios (Pandit et al., 2022; Peglion et al., 2022). Mammalian target of rapamycin (mTOR) activation inhibits apoptosome formation via upstream regulators, including growth factors, insulin levels, nutrients, metabolic status, and mechanical changes. In contrast, AMPK acts as an upstream regulator of this process (Li et al., 2024). The mTOR signaling pathway is a key pathway downstream of AMPK that regulates apoptosis. AMPK is able to negatively regulate mTOR activity by direct phosphorylation, thereby inducing apoptosis (Wang et al., 2023). However, activation of AMPK can directly or indirectly inhibit the activity of mTOR, impede the phosphorylation of its downstream molecules p70 ribosomal S6 kinase 1 (S6K1, p70S6K1) and cysteine protease-3 (caspase-3), and interfere with the process of protein synthesis, which can lead to blockade of the cell cycle at G0/G1 phase; thus, tumors in the patient's body show growth stagnation or regression. Our results revealed that the AMPK inhibitor Compound c significantly inhibited AMPK activation, which provided increasing evidence that AMPK activation is required to suppress tumorigenesis.

AMPK is the guardian of cellular energy homeostasis, and mitochondria are important dynamic organelles that provide energy to the cell (Herzig and Shaw, 2018). Under normal conditions, mitochondria undergo constant fusion and fission to achieve homeostasis and maintain morphological and functional integrity (Chen et al., 2021). However, in the presence of cancer, the dynamic balance of mitochondria is disrupted, and mitochondria tend to undergo fission (Shiino et al., 2024). The inhibition of mitochondrial fission or promotion of mitochondrial fusion is a measure to ameliorate CRC. In the present study,

cotreatment with naringenin and 5-fluorouracil activated AMPK and increased intracellular ROS levels with a significant decrease in the MMP, suggesting that AMPK inhibition improved mitochondrial function. In addition, we found that an imbalance between mitochondrial fission and fusion occurred in CRC cells, and the naringenin intervention caused mitochondrial fusion (MFN2) to increase and fission (DRP1) to decrease in CRC cells to maintain the mitochondrial homeostatic balance. Recent studies have shown that AMPK strongly interacts with MFN2 for the treatment of disease (Hu et al., 2021b). In addition, the effect of herbal medicine on the fission of mitochondria was mediated by an AMPK activation-dependent decrease in the level of DRP1 (Tong et al., 2023). Our results showed that naringenin caused AMPK activation to increase mitochondrial fusion through the downregulation of DRP1 and up-regulation of MFN2 expression, which was even more pronounced in combination with 5-fluorouracil. Thus, AMPK activation stimulates mitochondrial fusion and inhibits mitochondrial fission, which may be the mechanism of action of naringenin and the combination of drugs for CRC treatment.

Mitochondria play a crucial role in the process of apoptosis, which involves the release of factors that induce apoptosis and the upregulation of proteins related to apoptosis. They act as the central hub for cellular metabolism and are essential in maintaining redox balance, impacting disease progression and the advancement of cancer. Within the Bcl-2 family are members that either promote or inhibit apoptosis, with their main function being the regulation of mitochondrial structure and signaling pathways for caspase activation (Schmitt et al., 2024). The anti-apoptotic Bcl2 protein is located in the outer membrane of the mitochondrial membrane and prevents the release of cytochrome C, while the pro-apoptotic protein Bax opposes Bcl2 by forming a complex with it. The fate of cells is determined by either the homodimer or monomer of Bcl-2, Bcl-xL. In our study, it was observed that naringenin induced apoptosis in CRC LoVo cells. The synergistic effect of naringenin and 5-fluorouracil was more pronounced in promoting apoptosis of CRC LoVo cells compared to using either compound alone. Naringenin triggers apoptosis in CRC by activating AMPK and enhancing levels of apoptotic markers (Caspase-9, Caspase-3, Bak).

In summary, by cell culture vitro andmouse models in vivo, we found that naringenin activates the AMPK signaling pathway and promotes mitochondrial fusion to induce apoptosis in CRC cells (Fig. 9). We showed that naringenin induced apoptosis and inhibited CRC growth in LoVo cells by regulating mitochondrial function through activation of the AMPK pathway, and that naringenin combined with 5-fluorouracil had a more significant effect. Naringenin increases AMPK and inhibits CRC growth by inhibiting the expression of the mitochondrial junction protein Miro1 and the mitochondrial fission protein DRP1, promoting the expression of the mitochondrial fusion protein MFN2, and down-regulating the kinesin KIF5B, resulting in an increase in mitochondrial fusion and a decrease in fission, which is more pronounced in the

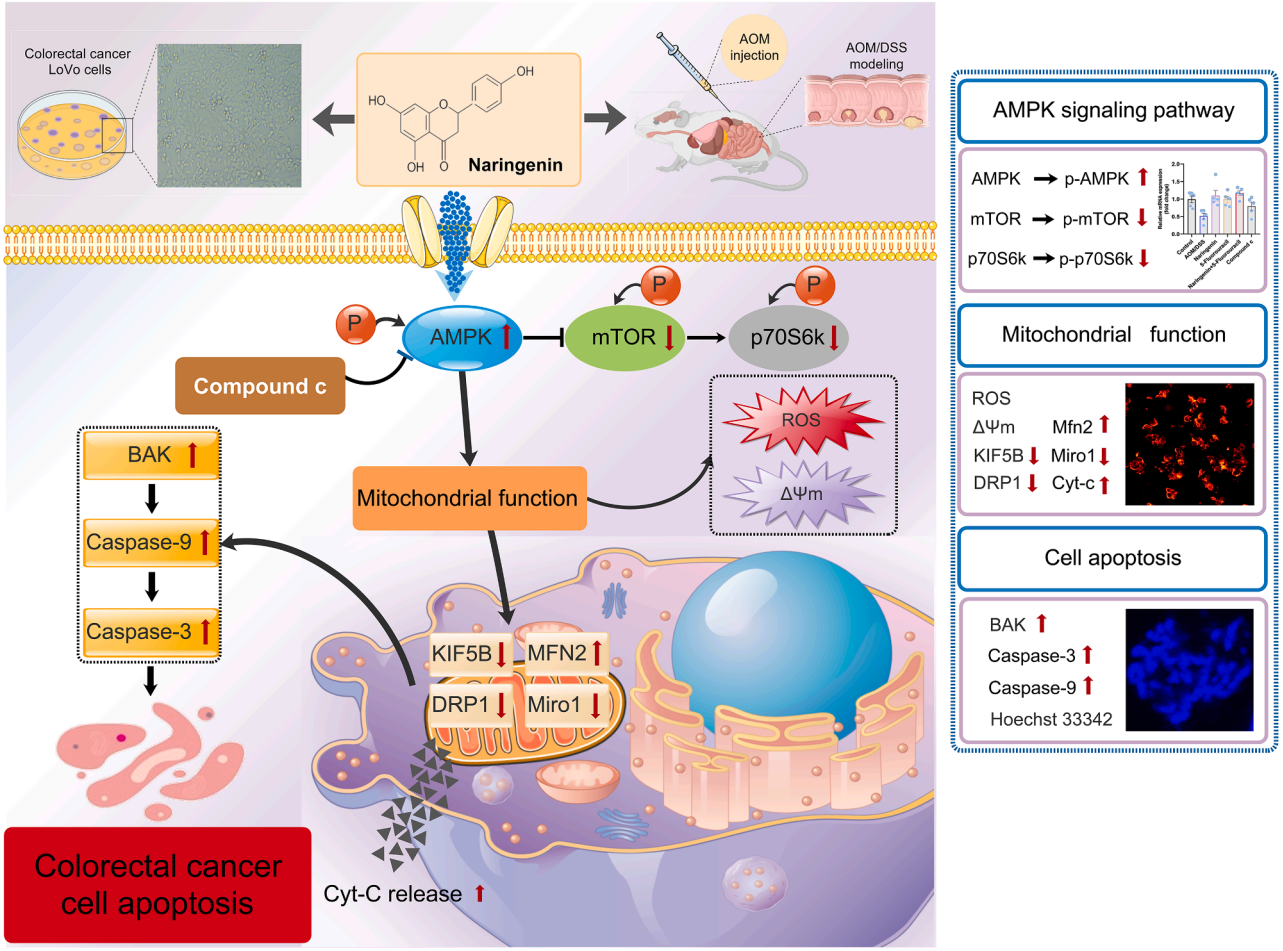

Fig. 9. Schematic diagram of naringenin-mediated regulation of metastasis and apoptosis in CRC cells through the AMPK and mitochondrial pathways. Using biological, pharmacological and morphological approaches at the animal, cellular and molecular levels, naringenin increased AMPK levels and Compound c inhibited AMPK by regulating AMPK expression at the animal and cellular levels. Then, the expression of mitochondrial fission (DRP1)- and fusion (MFN2)-related proteins in CRC cells was examined by detecting the expression of Miro1 and KIF5 to characterize the mitochondrial pathway. The expression of the DRP1- and MFN2-related proteins Miro1 and KIF5 was used to characterize mitochondrial transport, and the analysis of mitochondrial functions (changes in the mitochondrial membrane potential and ROS levels) provided new insights into the mechanism of metastasis and apoptosis in CRC.

combination of naringenin and 5-fluorouracil. Naringenin probably activates the AMPK signaling pathway, decreases mitochondrial membrane electric potential and increases ROS, thus promoting the apoptosis of CRC cells and exerting anti-rectal cancer effects, and the effects of naringenin combined with 5-fluorouracil are more significant.

In recent years, newly emerging targeted therapies and immunotherapies have drug side effects and limitations in their targets of action; therefore, it is also worth exploring whether naringenin can be combined with the targeted therapies and immunotherapies to improve patient outcomes. Naringenin has poor water solubility and low bioavailability, which affects its intestinal absorption. Combined nanotechnology has been proposed to overcome this challenge and improve the pharmacokinetics of naringenin, but few studies have analyzed the application of naringenin in CRC, and the efficacy of this approach and its safety need to be compared. Moreover, most of the current studies have focused only on in vitro cell lines and mouse models, and researchers do not yet know whether universal efficacy can be achieved in a wide range of patients; therefore, the antitumor effect of naringenin urgently needs further clinical data for further verification.

In our research, we investigate the influence of naringenin and its combination with chemotherapy agents on CRC, aiming to clarify the underlying molecular mechanisms. This study offers a novel perspective on the pathogenesis and metastatic processes of CRC, with the goal of mitigating the toxic and adverse effects of chemotherapy. Furthermore, we seek to identify innovative therapeutic targets for the treatment of CRC. By examining the synergistic effects of natural compounds in conjunction with chemotherapy, we strive to enhance apoptosis in CRC cells while minimizing the damage to vital organs such as the heart and liver. Our research also explores novel treatment approaches and their potential clinical applications for CRC therapy. In the subsequent phase of our study, the research team will focus on assessing the impact and mechanisms of action of naringenin encapsulated in nanocarriers, as well as the combination of nanocarrier-coated naringenin with 5-fluorouracil, on CRC. The objective is to augment the therapeutic efficacy and bioavailability of naringenin as a prospective clinical treatment, while diminishing the side effects and enhancing the therapeutic efficacy of chemotherapeutic agents.

Conclusions

We found that naringenin combined with 5-fluorouracil inhibited CRC more significantly than naringenin by activating AMPK signaling and regulating mitochondrial fusion and fission to inhibit CRC. Our study provides evidence for the inhibitory role of naringenin in CRC. We hope that in the future, basic research and clinical trials of naringenin or naringenin combined with 5-fluorouracil in CRC will be actively conducted to promote the development of highly effective and safe drugs that allow CRC patients to receive a truly individualized diagnosis and precise treatment.

Author contributions

All data were generated in house, and no paper mill was used. All authors agree to be accountable for all aspects of the work, ensuring its integrity and accuracy.

Supplementary materials: Supplementary materials associated with this article can be found in the online version at the Phytomedicine website.

CRediT authorship contribution statement

Dan Wang: Writing – original draft, Validation, Methodology, Investigation, Formal analysis, Data curation, Conceptualization. **Yue Zhou:** Investigation, Formal analysis, Data curation. **Li Hua:** Supervision, Methodology, Investigation. **Meichun Hu:** Software, Resources, Investigation, Formal analysis. **Ni Zhu:** Supervision, Software, Resources. **Yifei Liu:** Writing – review & editing, Visualization, Validation, Supervision, Methodology. **Yanhong Zhou:** Writing – review & editing, Project administration, Funding acquisition.

Declaration of competing interest

We declare that this manuscript entitled “The role of the natural compound naringenin in AMPK-mitochondria modulation and colorectal cancer inhibition ” which we submitted to Phytomedicine was original research and has not been published previously, and not under consideration for publication elsewhere, in whole or in part. All the authors listed agreed the manuscript for publication in Phytomedicine. All the authors declare that there are no conflicts of interest regarding the publication of this paper.

Acknowledgments

This research was funded by the Health Commission Health Project of Hubei Province (No. WJ2023M118) and Research and Innovation Team Project of Hubei University of Science and Technology (No. 2023T09).

Supplementary materials

Supplementary material associated with this article can be found, in the online version, at doi:10.1016/j.phymed.2024.155786.

References

Abdulrahman, R.M., Boon, M.R., Sips, H.C., Guigas, B., Rensen, P.C., Smit, J.W., Hovens, G.C., 2014. Impact of Metformin and compound C on NIS expression and iodine uptake in vitro and in vivo: a role for CRE in AMPK modulation of thyroid function. Thyroid 24, 78–87.

Chen, C., Qin, H., Tang, J., Hu, Z., Tan, J., Zeng, L., 2021. USP30 protects against oxygen-glucose deprivation/reperfusion induced mitochondrial fragmentation and ubiquitination and degradation of MFN2. Aging 13, 6194–6204.

Chen, J.F., Wu, S.W., Shi, Z.M., Hu, B., 2023. Traditional Chinese medicine for colorectal cancer treatment: potential targets and mechanisms of action. Chin. Med. 18, 14.

Chen, Q., Liu, Y., Zhu, Y., Zhu, Z., Zou, J., Pan, Y., Lu, Y., Chen, W., 2024. Cryptotanshinone inhibits PFK-mediated aerobic glycolysis by activating AMPK pathway leading to blockade of cutaneous melanoma. Chin. Med. 19, 45.

Chen, Y., Liu, Y., Zhou, Y., You, H., 2019. Molecular mechanism of LKB1 in the invasion and metastasis of colorectal cancer. Oncol. Rep. 41, 1035–1044.

Cheng, Z., Tu, J., Wang, K., Li, F., He, Y., Wu, W., 2024. Wogonin alleviates NLRP3 inflammasome activation after cerebral ischemia-reperfusion injury by regulating AMPK/SIRT1. Brain Res. Bull. 207, 110886.

Chou, T.C., 2010. Drug combination studies and their synergy quantification using the Chou-Talalay method. Cancer Res. 70, 440–446.

Fan, J., Yu, H., Lu, X., Xue, R., Guan, J., Xu, Y., Qi, Y., He, L., Yu, W., Abay, S., Li, Z., Huo, S., Li, L., Lv, M., Li, W., Chen, W., Han, B., 2023. Overlooked spherical nanoparticles exist in plant extracts: from mechanism to therapeutic applications. ACS Appl. Mater. Interfaces.

Fenton, A.R., Jongens, T.A., Holzbaur, E.L.F., 2021. Mitochondrial dynamics: shaping and remodeling an organelle network. Curr. Opin. Cell Biol. 68, 28–36.

Firouzi Amoodizaj, F., Baghaeifar, S., Taheri, E., Farhoudi Sefidan Jadid, M., Safi, M., Seyyed Sani, N., Hajazimian, S., Isazadeh, A., Shanehbandi, D., 2020. Enhanced anticancer potency of doxorubicin in combination with curcumin in gastric adenocarcinoma. J. Biochem. Mol. Toxicol. 34, e22486.

Gumushan Aktas, H., Akgun, T., 2018. Naringenin inhibits prostate cancer metastasis by blocking voltage-gated sodium channels. Biomed. Pharmacother. 106, 770–775.

Gupta, N., Zhang, B., Zhou, Y., McCormack, F.X., Ingledue, R., Robbins, N., Kopras, E.J., McMahan, S., Singla, A., Swigris, J., Cole, A.G., Holz, M.K., 2023. Safety and Efficacy of Combined Resveratrol and Sirolimus in Lymphangioleiomyomatosis. Chest 163, 1144–1155.

Herzig, S., Shaw, R.J., 2018. AMPK: guardian of metabolism and mitochondrial homeostasis. Nat. Rev. Mol. Cell Biol. 19, 121–135.

Hsu, C.C., Zhang, X., Wang, G., Zhang, W., Cai, Z., Pan, B.S., Gu, H., Xu, C., Jin, G., Xu, X., Manne, R.K., Jin, Y., Yan, W., Shao, J., Chen, T., Lin, E., Ketkar, A., Eoff, R., Xu, Z.G., Chen, Z.Z., Li, H.Y., Lin, H.K., 2021. Inositol serves as a natural inhibitor of mitochondrial fission by directly targeting AMPK. Mol. Cell 81, 3803–3819.e3807.

Hsu, L.C., Kuo, C.Y., Hsu, F.T., Chang, H.F., Ou, J.J., 2023. Hyperforin suppresses oncogenic kinases and induces apoptosis in colorectal cancer cells. In Vivo 37, 182–189.

Hu, G., Cao, C., Deng, Z., Li, J., Zhou, X., Huang, Z., Cen, C., 2021a. Effects of matrine in combination with cisplatin on liver cancer. Oncol. Lett. 21, 66.

Hu, X., Yang, Z., Liu, W., Pan, Z., Zhang, X., Li, M., Liu, X., Zheng, Q., Li, D., 2020. The anti-tumor effects of p-coumaric acid on melanoma A375 and B16 cells. Front. Oncol. 10, 558414.
Hu, Y., Chen, H., Zhang, L., Lin, X., Li, X., Zhuang, H., Fan, H., Meng, T., He, Z., Huang, H., Gong, Q., Zhu, D., Xu, Y., He, P., Li, L., Feng, D., 2021b. The AMPK-MFN2 axis regulates MAM dynamics and autophagy induced by energy stresses. Autophagy 17, 1142–1156.
Huang, X., Ke, K., Jin, W., Zhu, Q., Zhu, Q., Mei, R., Zhang, R., Yu, S., Shou, L., Sun, X., Feng, J., Duan, T., Mou, Y., Xie, T., Wu, Q., Sui, X., 2022. Identification of genes related to 5-fluorouracil based chemotherapy for colorectal cancer. Front. Immunol. 13, 887048.
Kaczanowski, S., 2016. Apoptosis: its origin, history, maintenance and the medical implications for cancer and aging. Phys. Biol. 13, 031001.
Khaled, S.S., Soliman, H.A., Abdel-Gabbar, M., Ahmed, N.A., Attia, K., Mahran, H.A., El-Nahass, E.S., Ahmed, O.M., 2022. The preventive effects of naringin and naringenin against paclitaxel-induced nephrotoxicity and cardiotoxicity in male wistar rats. Evid. Based Complement. Alternat. Med. 2022, 8739815.
Li, H., Zhu, F., Chen, H., Cheng, K.W., Zykova, T., Oi, N., Lubet, R.A., Bode, A.M., Wang, M., Dong, Z., 2014. 6-C-(E-phenylethenyl)-naringenin suppresses colorectal cancer growth by inhibiting cyclooxygenase-1. Cancer Res. 74, 243–252.
Li, R.Z., Guan, X.X., Wang, X.R., Bao, W.Q., Lian, L.R., Choi, S.W., Zhang, F.Y., Yan, P.Y., Leung, E.L.H., Pan, H.D., Liu, L., 2023. Sinomenine hydrochloride bidirectionally inhibits progression of tumor and autoimmune diseases by regulating AMPK pathway. Phytomedicine 114, 154751.
Li, X.L., Zhou, J., Xia, C.J., Min, H., Lu, Z.K., Chen, Z.R., 2024. [Corrigendum] PRIMA-1 (met) induces autophagy in colorectal cancer cells through upregulation of the mTOR/AMPK-ULK1-Vps34 signaling cascade. Oncol. Rep. 51.
Lian, G.Y., Wang, Q.M., Mak, T.S., Huang, X.R., Yu, X.Q., Lan, H.Y., 2021. Inhibition of tumor invasion and metastasis by targeting TGF-β-Smad-MMP2 pathway with Asiatic acid and Naringenin. Mol. Ther. Oncolytics 20, 277–289.
Liu, D., Sica, M.S., Mao, J., Chao, L.F., Siewers, V., 2022. A p-Coumaroyl-CoA biosensor for dynamic regulation of naringenin biosynthesis in saccharomyces cerevisiae. ACS Synth. Biol. 11, 3228–3238.
Liu, G., Wang, F., Feng, Y., Tang, H., 2024. Metformin inhibits NLRP3 inflammasome expression and regulates inflammatory microenvironment to delay the progression of colorectal cancer. Recent Pat Anticancer Drug Discov.
Liu, X., Zhao, T., Shi, Z., Hu, C., Li, Q., Sun, C., 2023. Synergism antiproliferative effects of apigenin and naringenin in NSCLC cells. Molecules 28.
Lu, Z., Wang, H., Ishfaq, M., Han, Y., Zhang, X., Li, X., Wang, B., Lu, X., Gao, B., 2023. Quercetin and AMPK: a dynamic duo in alleviating MG-induced inflammation via the AMPK/SIRT1/NF-κB pathway. Molecules 28.
Ma, Y., Li, C., Han, F., Liu, Y., Hani, U.E., Zhong, Y., Huang, D., Chen, W., Qian, H., 2024. Oral delivery of berberine by liver-targeted zwitterionic nanoparticles to overcome multi-intestinal barriers and extend insulin treatment duration. Chem. Eng. J. 485, 150129.
Maphetu, N., Unuofin, J.O., Masuku, N.P., Olisah, C., Lebelo, S.L., 2022. Medicinal uses, pharmacological activities, phytochemistry, and the molecular mechanisms of Punica granatum L. (pomegranate) plant extracts: a review. Biomed. Pharmacother. 153, 113256.
Martínez-Rodríguez, O.P., González-Torres, A., Álvarez-Salas, L.M., Hernández-Sánchez, H., García-Pérez, B.E., Thompson-Bonilla, M.D.R., Jaramillo-Flores, M.E., 2020. Effect of naringenin and its combination with cisplatin in cell death, proliferation and invasion of cervical cancer spheroids. RSC Adv. 11, 129–141.
Memariani, Z., Abbas, S.Q., Ul Hassan, S.S., Ahmadi, A., Chabra, A., 2021. Naringin and naringenin as anticancer agents and adjuvants in cancer combination therapy: Efficacy and molecular mechanisms of action, a comprehensive narrative review. Pharmacol. Res. 171, 105264.
Olivier, S., Diounou, H., Pochard, C., Frechin, L., Durieu, E., Foretz, M., Neunlist, M., Rolli-Derkinderen, M., Viollet, B., 2022. Intestinal epithelial AMPK deficiency causes delayed colonic epithelial repair in DSS-induced colitis. Cells 11.
Pandit, M., Timilshina, M., Gu, Y., Acharya, S., Chung, Y., Seo, S.U., Chang, J.H., 2022. AMPK suppresses Th2 cell responses by repressing mTORC2. Exp. Mol. Med. 54, 1214–1224.
Peglion, F., Capuana, L., Perfettini, I., Boucontet, L., Braithwaite, B., Colucci-Guyon, E., Quissac, E., Forsberg-Nilsson, K., Llense, F., Etienne-Manneville, S., 2022. PTEN inhibits AMPK to control collective migration. Nat. Commun. 13, 4528.
Rani, I., Kumar, S., Sharma, B., Prasad, R., Kaur, S., Sharma, P., Agnihotri, N., 2021. Elucidation of underlying molecular mechanism of 5-Fluorouracil chemoresistance and its restoration using fish oil in experimental colon carcinoma. Mol. Cell. Biochem. 476, 1517–1527.
Schmitt, L., Lechtenberg, I., Drießen, D., Flores-Romero, H., Skowron, M.A., Sekeres, M., Hoppe, J., Krings, K.S., Llewellyn, T.R., Peter, C., Stork, B., Qin, N., Bhatia, S., Nettersheim, D., Fritz, G., García-Sáez, A.J., Müller, T.J.J., Wesselborg, S., 2024. Novel meriolin derivatives activate the mitochondrial apoptosis pathway in the presence of antiapoptotic Bcl-2. Cell Death Discov. 10, 125.
Shi, X., Luo, X., Chen, T., Guo, W., Liang, C., Tang, S., Mo, J., 2021. Naringenin inhibits migration, invasion, induces apoptosis in human lung cancer cells and arrests tumour progression in vitro. J. Cell. Mol. Med. 25, 2563–2571.
Shiino, H., Tashiro, S., Hashimoto, M., Sakata, Y., Hosoya, T., Endo, T., Kojima, H., Tamura, Y., 2024. Chemical inhibition of phosphatidylcholine biogenesis reveals its role in mitochondrial division. iScience 27, 109189.
Siegel, R.L., Miller, K.D., Wagle, N.S., Jemal, A., 2023a. Cancer statistics, 2023. CA Cancer J. Clin. 73, 17–48.
Siegel, R.L., Wagle, N.S., Cercek, A., Smith, R.A., Jemal, A., 2023b. Colorectal cancer statistics, 2023. CA Cancer J. Clin. 73, 233–254.
Slika, H., Mansour, H., Wehbe, N., Nasser, S.A., Iratni, R., Nasrallah, G., Shaito, A., Ghaddar, T., Kobeissy, F., Eid, A.H., 2022. Therapeutic potential of flavonoids in cancer: ROS-mediated mechanisms. Biomed. Pharmacother. 146, 112442.
Tong, W., Leng, L., Wang, Y., Guo, J., Owusu, F.B., Zhang, Y., Wang, F., Li, R., Li, Y., Chang, Y., Wang, Y., Wang, Q., 2023. Buyang huanwu decoction inhibits diabetes-accelerated atherosclerosis via reduction of AMPK-Drp1-mitochondrial fission axis. J. Ethnopharmacol. 312, 116432.
Wai, T., Langer, T., 2016. Mitochondrial Dynamics and Metabolic Regulation. Trends Endocrinol. Metab. 27, 105–117.
Wang, S., Qiu, J., Liu, L., Su, C., Qi, L., Huang, C., Chen, X., Zhang, Y., Ye, Y., Ding, Y., Liang, L., Liao, W., 2020. CREB5 promotes invasiveness and metastasis in colorectal cancer by directly activating MET. J. Exp. Clin. Cancer Res. 39, 168.
Wang, X.H., Shen, C.P., Wang, T.T., Huang, Y., Jin, Y., Zhou, M.Y., Zhang, M.Y., Gu, S.L., Wang, M.Q., Liu, Z.C., Li, R., Cai, L., 2024. Shikonin suppresses rheumatoid arthritis by inducing apoptosis and autophagy via modulation of the AMPK/mTOR/ULK-1 signaling pathway. Phytomedicine 128, 155512.
Wang, Y., Dong, Y., Zhang, W., Wang, Y., Jao, Y., Liu, J., Zhang, M., He, H., 2023. AMPK/mTOR/p70S6K axis prevents apoptosis of Porphyromonas gingivalis-infected gingival epithelial cells via Bad(Ser136) phosphorylation. Apoptosis 28, 1012–1023.
Wang, Y., Wang, Z., Yang, H., Chen, S., Zheng, D., Liu, X., Jiang, Q., Chen, Y., 2022. Metformin ameliorates chronic colitis-related intestinal fibrosis via inhibiting TGF-β1/Smad3 signaling. Front. Pharmacol. 13, 887497.
Wittwer, N.L., Staudacher, A.H., Liapis, V., Cardarelli, P., Warren, H., Brown, M.P., 2023. An anti-mesothelin targeting antibody drug conjugate induces pyroptosis and ignites antitumor immunity in mouse models of cancer. J. Immunother. Cancer 11.
Xu, J., Guo, Z., Yuan, S., Li, H., 2022. BCL2L1 is identified as a target of naringenin in regulating ovarian cancer progression. Mol. Cell. Biochem. 477, 1541–1553.
Yang, Q., Zhang, X., Qin, H., Luo, F., Ren, J., 2022. Phenolic acid profiling of lactarius hatsudake extracts, anti-cancer function and its molecular mechanisms. Foods 11.
Zadra, G., Batista, J.L., Loda, M., 2015. Dissecting the dual role of AMPK in cancer: from experimental to human studies. Mol. Cancer Res. 13, 1059–1072.
Zhang, D., Man, D., Lu, J., Jiang, Y., Ding, B., Su, R., Tong, R., Chen, J., Yang, B., Zheng, S., Chen, D., Wu, J., 2023. Mitochondrial TSPO Promotes Hepatocellular Carcinoma Progression through Ferroptosis Inhibition and Immune Evasion. Adv. Sci., e2206669
Zhang, L., Xiao, Y., Yang, R., Wang, S., Ma, S., Liu, J., Xiao, W., Wang, Y., 2021. Systems pharmacology to reveal multi-scale mechanisms of traditional Chinese medicine for gastric cancer. Sci. Rep. 11, 22149.
Zhao, Y., Tan, H., Zhang, J., Zhan, D., Yang, B., Hong, S., Pan, B., Wang, N., Chen, T., Shi, Y., Wang, Z., 2024. Developing liver-targeted naringenin nanoparticles for breast cancer endocrine therapy by promoting estrogen metabolism. J. Nanobiotechnol. 22, 122.
Zhu, J., Chen, H., Guo, J., Zha, C., Lu, D., 2022. Sodium tanshinone IIA sulfonate inhibits vascular endothelial cell pyroptosis via the AMPK signaling pathway in atherosclerosis. J. Inflamm. Res. 15, 6293–6306.